https://doi.org/10.5194/egusphere-2026-2378
Preprint. Discussion started: 5 May 2026
© Author(s) 2026. CC BY 4.0 License.

Holocene-like summer climate during Marine Isotope Stage 11 in northwestern Greenland

John Michael N. Aguilar[1,2], Elizabeth K. Thomas[1]*, Diana S. Aga[2], Paul R. Bierman[3,4], Jason P. Briner[1], Isla S. Castañeda[5], Andrew J. Christ[3,a]

[1]Department of Earth Sciences, University at Buffalo, The State University of New York, Buffalo, NY, 14260, USA

[2]Department of Chemistry, University at Buffalo, The State of University of New York, Buffalo, NY, 14260, USA

[3]Rubenstein School of the Environment and Natural Resources, University of Vermont, Burlington, VT 05401, USA

[4]Gund Institute for Environment, University of Vermont, Burlington, VT 05401, USA

[5]Department of Earth, Geographic and Climate Sciences, University of Massachusetts, Amherst, MA 01002, USA

[a]currently at: U.S. Reinsurance Analytics, Aon plc, Denver, CO 80206, USA

*Corresponding author: Elizabeth K. Thomas (ekthomas@buffalo.edu)

Key Points:

1. MIS 11 in northwestern Greenland had similar summer temperature to peak Holocene conditions across Greenland
2. Holocene-like MIS 11 conditions suggest that sustained moderate warmth can drive major Greenland Ice Sheet loss
3. ^{2}H-enriched summer vapor during MIS 11 due to greater local evapotranspiration, consistent with reduced ice extent and expanded vegetation

Keywords: Camp Century, Marine Isotope Stage 11, Greenland Ice Sheet

https://doi.org/10.5194/egusphere-2026-2378
Preprint. Discussion started: 5 May 2026
© Author(s) 2026. CC BY 4.0 License.

Abstract

Determining the climatic conditions under which the Greenland Ice Sheet (GrIS) was smaller than present is important to quantify GrIS sensitivity to climate change. We use biomarkers in sediment collected beneath the GrIS at Camp Century, northwestern Greenland to reconstruct summer temperature and atmospheric circulation 416,000 ± 38,000 years ago (Marine Isotope Stage 11; MIS 11). We find that northwestern Greenland summer climate during MIS 11 was similar to the middle Holocene but different than the 20th century: air temperature was 4.7 ± 3.2°C warmer and atmospheric water vapor isotope values were 22 ± 18 ‰ ^{2}H-enriched, indicating a greater contribution of locally evapotranspired moisture. These conditions are similar to or slightly warmer than during peak Holocene warmth on Greenland, when the Camp Century site remained ice-covered, and cooler than the Last Interglacial (LIG). Biomarkers from lower in the section likely represent an earlier ice-free interval, potentially during the Pliocene or early Pleistocene, and record climatic conditions similar to MIS 11. These data add to the sparse available climate data for the early and middle Pleistocene on Greenland, and suggest interglacial periods had similar temperature throughout the Pleistocene. We interpret the reduced GrIS extent in northwestern Greenland during MIS11 compared to the Holocene, despite similar temperature, to indicate ice-sheet response to prolonged warmth, as reconstructed in southern Greenland. Therefore, efforts to reduce both the magnitude and duration of summer warmth in the coming centuries will be important to curbing ice-sheet retreat.

Plain Language Summary

As the Arctic warms rapidly, the Greenland Ice Sheet (GrIS) is losing mass, with implications for global sea levels. Quantifying past climate for periods when the GrIS was smaller than

https://doi.org/10.5194/egusphere-2026-2378
Preprint. Discussion started: 5 May 2026
© Author(s) 2026. CC BY 4.0 License.

present can constrain how it may respond to future warming. We studied biomarkers in sediments recovered from beneath 1387 m of ice at Camp Century, northwestern Greenland. These sediments were deposited when the ice sheet was smaller than today. We reconstructed summer temperature and summer precipitation stable isotope values, which indicate how far that moisture traveled before landing at the site, during a period of reduced ice sheet size at 400,000 years ago. Our results showed that summers were ~4.7°C warmer than today and that local moisture contributed more to precipitation, likely due to reduced ice cover and increased vegetation. These conditions are similar to those experienced during the most recent warm period in geologic history, when the GrIS remained large enough to cover the Camp Century site. Yet, 400,000 years ago, the site was ice-free, suggesting that the retreat was likely caused by prolonged moderate warmth. This result highlights the need to limit both how warm and how long future warming lasts to reduce ice loss.

1. Introduction

Quantifying the sensitivity of the Greenland Ice Sheet (GrIS) to climate is an important challenge, as the GrIS contains 7.4 m sea level equivalent and the Arctic is in a rapidly warming part of the planet (Aschwanden et al., 2019; Smith et al., 2020). Ocean warming may cause rapid recession of calving glaciers, some of which are sourced from near the center of the GrIS (Callard et al., 2025; Guo et al., 2019; Holland et al., 2008). Yet, much of the GrIS bed is above sea level and should be resilient to ocean forcing (Morlighem et al, 2017). Atmospheric warming also causes ice-sheet mass loss, and although greater snowfall may partially offset this melt, the elevation-albedo feedback could push the GrIS beyond a threshold of irreversible demise (Fyke et al., 2018). Although we have observations of atmospheric temperature, they span only the past few decades and represent conditions cooler than those predicted for the future. As a result, contemporary data provide limited constraints on the long-term GrIS response to atmosphere and ocean forcing (Box et al., 2009; Nowicki et al., 2016; Jensen, 2025).

https://doi.org/10.5194/egusphere-2026-2378
Preprint. Discussion started: 5 May 2026
© Author(s) 2026. CC BY 4.0 License.

Reconstructing temperature and atmospheric circulation near the margins of the GrIS during past periods of reduced ice sheet size can highlight mechanisms influencing GrIS change today. Yet, the modern GrIS covers sediment archives deposited during such periods, and many others that may have once existed along the fringes of Greenland were eroded by subsequent glaciations. Here we present new lipid biomarker data from subglacial sediments at Camp Century that constrain past temperature and atmospheric circulation during Marine Isotope Stage (MIS) 11 in northwestern Greenland and evaluate these results in the context of existing marine, ice-core, and terrestrial paleoclimate records.

1.1. Interglacial Climate in Greenland

Climate on Greenland is intimately linked with global heat transport, as Greenland lies between areas of North Atlantic Deep Water formation (Bullister et al., 2013). The North Atlantic Ocean was relatively warm during the Pliocene (Lawrence et al., 2009). Cooling at the Plio-Pleistocene transition, which manifested during both interglacial and glacial periods at high latitudes, caused Northern Hemisphere ice-sheet growth and altered the global carbon cycle, forcing tropical and high-latitude temperature to be in step (Herbert et al., 2010; Lawrence et al., 2010). Through the Pleistocene, glacial periods became increasingly cold, whereas interglacial periods remained at similar temperature at both the high latitudes and the tropics (Herbert et al., 2010; Lawrence, et al., 2010). In the North Atlantic region, mid- to late-Pleistocene interglacial periods exhibited some temperature variability: Marine Isotope Stages (MIS) 9 and 5 were up to ~1 to 2°C warmer than the Holocene, MIS 11 had similar temperature to the Holocene but was much longer, and MIS 7 and 13 were approximately 1°C cooler than the Holocene (Cluett & Thomas, 2021; de Vernal & Hillaire-Marcel, 2008; Irvalı et al., 2020). This contrasts with the eastern Arctic, which experienced ‘super interglacial’, i.e., extreme, warmth during MIS 11, with similar timing to warmth in the Southern Ocean and Antarctica (Melles et al., 2012).

https://doi.org/10.5194/egusphere-2026-2378
Preprint. Discussion started: 5 May 2026
© Author(s) 2026. CC BY 4.0 License.

The highest-resolution climate time series for Greenland are derived from ice cores, some of which span both MIS 1 (the Holocene) and parts of MIS 5 (the Last Interglacial, LIG). These time series suggest that mean annual temperature was 2 to 3°C warmer than modern during peak Holocene warmth (Kobashi et al., 2017; Martin et al., 2024) and 8 ± 4°C warmer during peak LIG warmth (Dahl-Jensen et al., 2013). Yet these ice-core time series are annual averages for high elevation and likely do not closely reflect summer temperature at the ice sheet margins, which governs ablation and in turn impacts ice-sheet mass balance.

A reanalysis product using spatial and seasonal information from a climate model and temporal information from ice-core proxy time series found that middle Holocene Greenland-wide summers were 3.6 ± 0.4°C higher than present (Buizert et al., 2018). Peak Holocene summer temperature around the ice-sheet margins, inferred from biomarkers and insect fossils in lacustrine sediment archives, were 2 to 9°C higher than present from 11.7 to 5.0 ka, with some evidence for greater warming in northern Greenland compared to southern Greenland (Acharya et al., 2025; Axford et al., 2021; Axford et al., 2019; Axford et al., 2017; Axford et al., 2013; Briner et al., 2016; Cluett et al., 2023; McFarlin et al., 2018; Schneider et al., 2024; Thomas et al., 2018). Scattered sediment sections and one extant lake contain pre-Holocene interglacial material with fossils that suggest LIG July temperature was 4.5 to 9.5°C higher than present (Bennike & Böchner, 1992, 1994; Broderson & Bennike, 2003; Hedenäs, 1994; Hedenäs & Bennike, 2003; McFarlin et al., 2018) and Plio-Pleistocene summer temperatures 6.5 to 8.5°C higher than present (Atti et al., 2024; Bennike, 1990; Bennike et al., 2002; Bennike et al., 2023; Bennike et al., 2010).

The GrIS is additionally sensitive to moisture supply. Time series of water cycle change suggest that the middle Holocene experienced greater winter snowfall and more locally-sourced summer precipitation (Balascio et al., 2013; Thomas et al., 2016; Thomas et al., 2020), and may have had drier summers compared to present (Aebly & Fritz, 2009; Anderson & Leng, 2004).

https://doi.org/10.5194/egusphere-2026-2378
Preprint. Discussion started: 5 May 2026
© Author(s) 2026. CC BY 4.0 License.

There is therefore evidence that from 11.7 to 5.0 ka the terrestrial margins of Greenland were warmer than present, with periods of greater snowfall.

Together, these records demonstrate moderate to pronounced warmth in Greenland during interglacial periods, yet significant uncertainties remain. Proxies differ in their seasonal sensitivity, variously capturing peak summer conditions (i.e., July temperature), temperature of the months above freezing, or annual mean temperature (Bennike, 1990; Francis et al., 2006; Otiniano et al., 2024; Raberg et al., 2021). These differences complicate direct inter-proxy comparisons of inferred temperature magnitudes. In addition, the impact of polar amplification, which is the phenomenon whereby temperature changes more rapidly at high latitudes compared to low latitudes due to positive feedbacks, including the sea ice-albedo feedback (Bekryaev et al., 2010; Miller et al., 2010), has not been systematically assessed across available time series. Finally, climate during pre-Holocene warm periods is poorly constrained due to sparse records, limiting our ability to evaluate the duration, magnitude, and spatial extent of Greenland climate during periods when the GrIS was smaller than present.

1.2. Constraints on Greenland Ice Sheet Extent during Warm Periods

Understanding the implications of past warmth for the GrIS requires knowledge of past GrIS extent. Northern Hemisphere ice sheets grew large enough to deliver significant ice-rafted debris to the surrounding oceans at 2.7 Million years (Ma) (Jansen et al., 2000; Larsen et al., 1994; Raymo et al., 1987; Raymo et al., 1989; Shackleton et al., 1984; St. John & Krissek, 2002). The most direct evidence for GrIS size is from rock beneath the GISP2 ice core, which suggests this site must have been glaciated for at least 820 kyr during the past 1.1 Ma (Bierman et al., 2024a; Schaefer et al., 2016). Continuous time series from marine sediment archives suggest that the GrIS persisted through mid- to late-Pleistocene interglacial periods (Hatfield et al., 2016; Reyes et al., 2014). The southern dome of the GrIS was likely smaller during the

https://doi.org/10.5194/egusphere-2026-2378
Preprint. Discussion started: 5 May 2026
© Author(s) 2026. CC BY 4.0 License.

prolonged but mild MIS11, but appears to have persisted through brief, warmer interglacials (MIS9, MIS5), perhaps because their warm intervals were of insufficient duration to cause substantial retreat (Cluett & Thomas, 2021; de Vernal & Hillaire-Marcel, 2008; Irvalı et al., 2020).

The minimum GrIS extent during the Middle Holocene has been constrained using proglacial-threshold lakes and reworked marine shells deposited in moraines (Briner et al., 2010; Weidick & Bennike, 2007). This evidence suggests that the timing and size of the GrIS minimum Holocene extent varied around the ice sheet but was generally only minimally reduced in size relative to present (Briner et al., 2014; Briner & Bennike, 2025; Cronauer et al., 2016; Larsen et al., 2015; Tabone et al., 2024). The southwestern portion of the GrIS was likely the farthest behind its modern extent during the middle Holocene (Lecavalier et al., 2014), but more constraints from other regions are required to verify this assessment.

1.3. Gaps in Understanding Pre-Holocene Climate and Ice Sheet Response

The most detailed understanding of both climate and ice sheet extent in Greenland for a previous warm period is for the early and middle Holocene, a period with moderate warmth and moderate, albeit incompletely known, ice-sheet retreat. The greatest number of constraints of pre-Holocene ice-sheet size are from the more widely studied southern region of Greenland. Due to spatial heterogeneity, it is critical to quantify the ice-sheet response in northern Greenland to a range of interglacial conditions, both warmer and longer than the Holocene. It is also critical to quantify climate during pre-Holocene interglacials and assess the spatial expression and mechanisms influencing interglacial warmth. Sub-ice sedimentary archives offer a means to directly constrain the magnitude and timing of past ice-free periods and contain proxies to reconstruct terrestrial environmental conditions near the ice-sheet margins (Bierman et al., 2024a, 2024b; Christ et al., 2021; Christ et al., 2023; Collins et al., 2024).

https://doi.org/10.5194/egusphere-2026-2378
Preprint. Discussion started: 5 May 2026
© Author(s) 2026. CC BY 4.0 License.

This study constrains temperature and precipitation isotope values during the months above freezing for two periods when the ice sheet was smaller than present as recorded in basal sediments at Camp Century: MIS 11 and the Pliocene or Early Pleistocene (Bierman et al., 2024b). We use lipid biomarkers extracted from sub-ice sediments collected in 1966 (Text S1) (Christ et al., 2021; Bierman et al., 2024b; Collins et al., 2025). The biomarkers are distinctive of plants and bacterial communities that exist in extant ice-free areas and therefore had to have been produced under ice-free conditions. To place our findings in a broader spatial context, we also conduct a meta-analysis of published Greenland interglacial temperature and precipitation isotope values and assess the spatial patterns of warmth and water cycle change. This allows us to assess climate conditions during multiple interglacial periods when the GrIS was smaller than present.

2. Methods

2.1. Lipid Biomarker Extraction and Paleoclimate Reconstructions

We extracted, purified, and analyzed *n*-alkanoic acids (plant waxes) and glycerol dialkyl glycerol tetraethers (GDGTs) from the <64 μm grain size sediment fractions following established protocols (Thomas et al., 2023; Holtzman et al., 2025) (details in text S2 and Bierman et al., 2024b). We used the mean of two high-latitude lacustrine calibrations to infer air temperature of the months above freezing (MAF) from branched GDGTs (brGDGTs) (Otiniano et al., 2024; Raberg et al., 2021). The associated calibration errors are 2.14°C and 1°C (RMSE), respectively, and we propagated calibration uncertainty and analytical error into inferred temperature values (Text S3, Equations S1 and S2; Figure S4). We used these calibrations since they were derived from high-latitude Arctic lakes. We inferred lake water δ^2H values using the C_{22} *n*-alkanoic acid in Units 1 and Units 3 to 5 and an apparent fractionation value for aquatic plants in high-latitude lakes of -124 ± 5 ‰ (Dion-Kirschner et al., 2020; Gorbey et al.,

https://doi.org/10.5194/egusphere-2026-2378
Preprint. Discussion started: 5 May 2026
© Author(s) 2026. CC BY 4.0 License.

2022; Hollister et al., 2022) (Equation S7, Text S3.5). We infer leaf water δ^2H values from the C_{28} *n*-alkanoic acid in all five units using biosynthetic fractionation values for high-latitude terrestrial plants in bioclimate zones similar to northwestern Greenland of -143 ± 5 ‰ (O'Connor et al., 2020) (Equation S8, Text S3.5).

Because we have independent summer temperature and precipitation δ^2H reconstructions, we can account for the effects of local condensation temperature on summer precipitation δ^2H values, providing insights into the vapor δ^2H values of the airmasses arriving at the Camp Century site (Thomas et al., 2018; Holtzman et al., 2025) (Text S3.7). We calculated the temperature-dependent equilibrium fractionation factor (Clark & Fritz, 1997; Majoube, 1971) using brGDGT-inferred MAF temperature from the same samples as the leaf wax δ^2H measurements and then used the fractionation factor and inferred summer precipitation δ^2H values to estimate summer vapor δ^2H values in each sample (Equations S13 - S14).

2.2. Modern context: Elevation and lapse-rate corrections for comparison with observational data

To place inferred temperature and precipitation isotope values reconstructed from Camp Century sediments in context, we compare the results to modern observations. The nearest meteorological station with precipitation isotope observations is at Pituffik (Figure 1A) (IAEA/WMO, 2015; Hersbach et al., 2020). First, we lapse-rate adjusted the Pituffik temperature and precipitation isotope values (at 77 m above sea level, asl) to align with the elevation at which the Camp Century sediments were deposited, a value that we estimated as follows. Although the ice-sheet bed at Camp Century is 530 ± 30 m asl today (Morlighem et al., 2017), the land surface elevation would be 810 ± 60 m asl (280 ± 50 m higher than today) under an ice-free, fully isostatically adjusted crust (Paxman et al., 2022). Another possibility is that the GrIS was smaller than present but not entirely absent, leading to the possibility that the full

https://doi.org/10.5194/egusphere-2026-2378
Preprint. Discussion started: 5 May 2026
© Author(s) 2026. CC BY 4.0 License.

isostatic adjustment yields an elevation that is too high. Alternatively, the GrIS margin was inland of, but close to, the Camp Century site. In this case, a forebulge could have caused the elevation to be tens of meters higher than the full isostatic adjustment value (Brandes et al., 2025). This region in northwestern Greenland was influenced by the forebulges of the more massive Innuitian and Laurentide ice sheets (Caron et al., 2018). Given the possible elevation range between the present value of 530 ± 30 m, an isostatically adjusted value of 810 ± 60 m, or a forebulge value of tens of meters higher than 810 m, we assume that 810 ± 60 m is a likely elevation that includes uncertainty related to unknowns in ice-sheet size and the transient nature of elevation through the time when these sediments were emplaced.

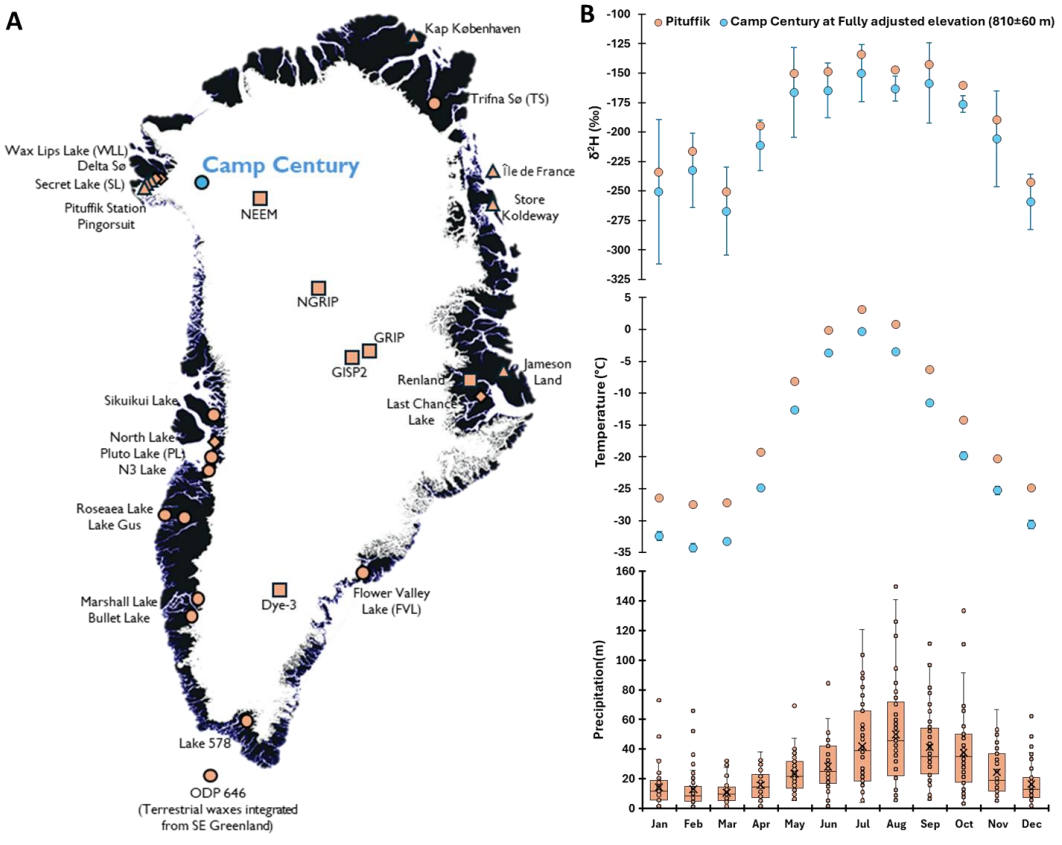

Figure 1. (A) Location (blue circle) of Camp Century (77.1667°N, -61.1333°E), Northwest Greenland and other sites mentioned in text. Orange symbols indicate the locations of sites

https://doi.org/10.5194/egusphere-2026-2378
Preprint. Discussion started: 5 May 2026
© Author(s) 2026. CC BY 4.0 License.

mentioned in text, including brGDGT and leaf wax (circles), chironomid assemblage (diamonds), ice core (squares), and plant macrofossil (triangles). (B) Pituffik Station (orange) and Camp Century derived via lapse-rate correction (Section 2.2, Text S3.4) (blue) monthly precipitation hydrogen isotope observations (δ^2H) (top, 1966 to 1969 CE) (IAEA/WMO, 2015), air temperature (middle, 1950 to 2000 CE) and precipitation amount (bottom, 1950 to 2000 CE) (Hersbach et al., 2020). δ^2H precipitation and temperature are monthly means; error bars incorporate interannual variability and elevation correction uncertainty (see methods). Precipitation plots illustrate mean (x'es), median and interquartile range (line and box), 5th and 95th percentile (whiskers), and outliers (dots).

We adjust the temperature and precipitation isotope values for the months above freezing at Pituffik from its elevation of 77 m asl to the Camp Century adjusted elevation of 810 m asl, incorporating 60 m of uncertainty into all calculations. We apply lapse rates established for low-elevation, high-latitude sites of -5 ± 1°C/km for summer (Fausto et al., 2009) and -46 ± 8 ‰ δ^2H/km (Koerner & Russell, 1979) (Equations S3 and S4). The 810 ± 60 m adjustment therefore equates to -4°C and -37 ‰, with elevation-related uncertainties of 1°C and 3 ‰. We report a mean-elevation adjusted temperature and precipitation anomaly relative to the late 20th century for each unit, and fully propagate uncertainties, including variance among Camp Century samples in each unit, interannual variance in modern observations, and uncertainties in analyses, lapse-rate, and elevation (Texts S3.1, 3.4, and 3.5).

2.3. Meta-analysis of published Greenland paleoclimate time series

We compiled published Greenland paleoclimate time series for comparison with the Camp Century data. For consistency, we determined the value of each time series relative to the same anomaly period, the late 20th century (Table S1 and S2). Herein, the anomaly period refers to observations from 1950–2000 CE, obtained from ERA5 via Climate Reanalyzer (Hersbach et al., 2020) except for ice-core sites, where modern temperature estimates were taken directly from datasets reported in the original ice-core studies (Buizert et al., 2018; Kobashi et al., 2017). We define 1950–2000 CE as our modern baseline, and refer to this period as "modern" throughout the rest of the text, as it represents a period with robust observational

https://doi.org/10.5194/egusphere-2026-2378
Preprint. Discussion started: 5 May 2026
© Author(s) 2026. CC BY 4.0 License.

coverage and aligns with the sampling period for precipitation isotope observations (IAEA/WMO, 2015).

These temperature data were used to identify months with mean temperatures above freezing at each study site. Modern precipitation isotope values were extracted from the Online Isotopes in Precipitation Calculator (OIPC), which provides globally calibrated long-term mean isotope fields based on observational data and spatial interpolation (Bowen, 2017; Bowen et al., 2005; IAEA/WMO, 2015). For each site, we calculated the mean modern precipitation isotope value for the months above freezing to allow direct comparison with proxy-derived precipitation isotope values for the months above freezing.

The biomarkers in the Camp Century samples likely represent mean climate of centuries to a few millennia. To enable direct comparison, we therefore calculated millennial-scale mean values of published paleoclimate time series. To determine peak Holocene temperature, we calculated the mean of the warmest two millennia between 11.7 and 5.0 ka in each dataset. For brGDGT time series, we used the same proxy-to-temperature calibration approach as for the Camp Century samples (section 2.1 and text S3.1). For chironomid time series, we used the chironomid-July air temperature calibration (Francis et al., 2006) to infer temperature, as that was consistently reported by all publications. For precipitation isotope time series, since some datasets do not have independent temperature constraints, we calculated the mean values for 8 to 5 ka, an interval that coincides with peak Holocene warmth on Greenland (Axford et al., 2021; Briner et al., 2016). We used the same plant wax fractionation factor approach to calculate lake and leaf water isotope values for all plant wax time series. Finally, we quantified uncertainties by propagating both the variability within each time series and the errors associated with calibrations.

https://doi.org/10.5194/egusphere-2026-2378
Preprint. Discussion started: 5 May 2026
© Author(s) 2026. CC BY 4.0 License.

To compare reconstructions of Greenland temperature based on different proxies, we must understand the seasonal bias of each proxy. brGDGTs reflect MAF temperature, whereas chironomids and plant macrofossils primarily reflect peak summer (July) air temperature (Bennike, 1990; Francis et al., 2006; Otiniano et al., 2024; Raberg et al., 2021). Analysis of modern seasonal temperature relationships at Pituffik Station, based on ERA5 data (Hersbach et al., 2020), shows that although July and MAF air temperatures are strongly and linearly correlated, MAF increases more slowly than July temperature (Figure S11). July temperature captures peak summer warmth, while MAF temperature incorporates all months with mean temperature above 0°C, including cooler shoulder-season months, and thus responds more weakly to the same forcing than July temperature. Therefore, chironomid or macrofossil-inferred July temperature anomalies of 7.0°C would be recorded by brGDGTs as a 4.5°C MAF temperature anomaly, assuming the modern relationship is constant through geological time. This is likely a poor assumption, since the length of the MAF season changes with climate, likely causing the MAF-July temperature relationship to change. We therefore do not convert from one seasonal value to another but note that the seasonal biases in proxies cause brGDGT temperature anomalies to be smaller than chironomid or macrofossil anomalies, even under the same climate conditions.

There are a few locations in Greenland with both precipitation isotope and temperature reconstructions (Acharya et al., 2025; Grootes and Stuiver, 1999; Kobashi et al., 2017; Thomas et al., 2020). To compare vapor isotope values at these locations with those reconstructed at Camp Century, we used the same approach applied to the Camp Century data for both the modern and Holocene observations, except for ice core time series, where we applied the fractionation factor for temperatures below freezing (Ellehoj et al., 2013). The isotope time series at Flower Valley and Secret lakes (Balascio et al., 2013; Lasher et al., 2017) do not have

https://doi.org/10.5194/egusphere-2026-2378
Preprint. Discussion started: 5 May 2026
© Author(s) 2026. CC BY 4.0 License.

independent temperature time series from the same lake, so we used inferred temperature from nearby sites (Text S3.7).

Once we have both the value for the late 20th century anomaly period and the mean value for the published paleoclimate time series, we calculate anomaly values as at Camp Century by calculating the difference between the Holocene, LIG, or Plio-Pleistocene mean values and the late 20th century value. We incorporated uncertainties from both the reconstructed time series and the modern reference dataset (Text S3.6, Table S1 and S2). The anomaly values presented here may differ from those reported in the original studies, as we use ERA5 temperature data from 1950 to 2000 CE and OIPC stable isotope values as the reference values for all sites, whereas the original studies may have used different time periods or sources for the modern anomaly value.

3. Proxy Systematics and Biomarker Interpretation

The lipid biomarkers preserved in the Camp Century sediments can provide information about past temperature and hydrologic conditions in northwestern Greenland. Interpreting the climatic signals from these biomarkers requires understanding the sources, depositional environments, and seasonal sensitivities influencing each proxy system. These factors control the environmental conditions recorded by each proxy and will allow us to identify the settings under which these biomarkers were produced and preserved. Here we report biomarker results from our samples and use measured distributions, isotope values, and published data from similar modern settings to evaluate the proxy systematics of GDGTs and plant wax *n*-alkanoic acids, including their production environments, seasonal biases, and the climatic variables they reflect. This framework provides the basis for reconstructing the temperature and hydrologic conditions recorded in the Camp Century sub-ice sediments at the time the biomarkers were produced.

https://doi.org/10.5194/egusphere-2026-2378
Preprint. Discussion started: 5 May 2026
© Author(s) 2026. CC BY 4.0 License.

3.1. GDGTs

Branched GDGTs are membrane lipids primarily produced by bacteria and are commonly found in soils and lake sediments (Sinninghe Damsté et al., 2000), whereas isoGDGTs are produced mainly by archaea, particularly ammonia-oxidizing Thaumarchaeota in aquatic and marine environments (Sinninghe Damsté et al., 2002). We detected brGDGTS and the isoprenoid GDGTs (isoGDGTs) crenarchaeol (cren) and caldarchaeol (cald) in all Camp Century samples. Abundances of the other isoGDGTs (GDGT-1, 2, 3, and crenarchaeol regioisomer) were generally below the detection limit, and the Branched to Isoprenoid Tetraether (BIT) index was >0.97 for all samples. Camp Century brGDGT distributions are most similar to brGDGTs from modern high-latitude lakes, rather than peats or soils (Figure S1 & S2) (Cluett et al., 2023; Lindberg et al., 2022; Martínez-Sosa et al., 2021; Naafs et al., 2017; Raberg et al., 2021; Russell et al., 2018;Thomas et al., 2018; Zhao et al., 2021), so we infer that the brGDGTs in all units in Camp Century were produced in aquatic settings. Independent classification using the BIGMaC algorithm (Martínez-Sosa et al., 2023) also suggests the Camp Century samples are from a lacustrine depositional environment, providing additional evidence for an lacustrine source of brGDGT production across all units.

Although it may seem counterintuitive that glacial sediments are dominated by lake-derived GDGTs, we explain this finding as follows: the modern ice-free landscape in northwestern Greenland is dotted with shallow lakes, in some areas covering more than 80% of the landscape (Walcott-George et al., 2025). It is therefore likely that the organic matter preserved in both the subglacial and proglacial units of the Camp Century sub-ice sediments, which integrate material from across the landscape overridden by the ice sheet, includes organic matter from lakes. The concentration of brGDGTs in modern lake sediments is five-fold higher than that in modern soils (Figure S10) (Guo et al., 2020; Hollister et al., 2022; Martínez-Sosa et

https://doi.org/10.5194/egusphere-2026-2378
Preprint. Discussion started: 5 May 2026
© Author(s) 2026. CC BY 4.0 License.

al., 2021). Lake-derived brGDGTs would therefore readily dominate the brGDGT distribution in a mixture of soil and lake sediments.

Lacustrine brGDGT production can be influenced by suboxic conditions, which may alter the distribution of high-abundance compounds and bias reconstructed temperatures by several degrees (Harning et al., 2025; Raberg et al., 2025). The cald/cren ratio in all Camp Century samples, however, was <10, indicating absence of suboxic conditions. We therefore applied two high-latitude lake-based calibrations (Otiniano et al., 2024; Raberg et al., 2021) (Equations S1 and S2; Figure S4) to estimate MAF air temperatures from Camp Century brGDGTs. These calibrations were selected because they were developed using Arctic Lake datasets, where brGDGT distributions exhibit the strongest sensitivity to mean MAF temperature (Otiniano et al., 2024; Raberg et al., 2021).

3.2. Plant wax δ^2H-inferred precipitation δ^2H and evaporation

We follow the PAGES Iso2k framework (Konecky et al., 2020) to structure our isotope proxy interpretation. We first define the measured proxy material and its inferred source (plant origin, seasonality, and source water for *n*-alkanoic acids), then interpret the controls on plant source-water δ^2H values, and finally link these to the climate mechanisms influencing precipitation δ^2H values.

3.2.1. Measured and Inferred Material: The Plant Source, Production Season, and Source Water for *n*-Alkanoic Acid Homologs

Determining the plant source of each plant wax homolog establishes the source-water pool for the plant wax hydrogens. All Camp Century samples contained C_{20} through C_{32} *n*-alkanoic acids, with C_{24}–C_{28} as the dominant chain-lengths, and Carbon Preference Index (CPI) > 2 (Equation S4). The long-chain C_{26} and C_{28} *n*-alkanoic acids contain similar trends in

https://doi.org/10.5194/egusphere-2026-2378
Preprint. Discussion started: 5 May 2026
© Author(s) 2026. CC BY 4.0 License.

concentration, $\delta^{13}C$ values, and $\delta^{2}H$ values in all five Camp Century units (Figure S6 and S9). Likewise, the mid-chain C_{20} and C_{22} *n*-alkanoic acids exhibited similar trends, which were distinct from the long-chain waxes in Unit 1 and Units 3-5, but similar to the trends in the long-chain waxes in Unit 2.

The diverging concentration and $\delta^{2}H$ trends between the mid- and long-chain waxes in all but Unit 2 in the Camp Century sediments suggest that these homologs come from different sources. In Unit 2, all chain lengths likely come from the same source. The C_{24} and C_{30} *n*-alkanoic acids display varying degrees of similarity with the other homologs. The C_{24} is likely from a mix of sources, and the C_{30} generally had high uncertainties for isotope measurements, due to its low concentration. The $\delta^{13}C$ values for C_{28} in all five Camp Century units overlap with $\delta^{13}C$ values of modern Arctic graminoids and shrubs, indicating a terrestrial source for this homolog (Hollister et al., 2022) (Figure S8). In contrast, the $\delta^{13}C$ values for C_{22} in all five Camp Century units overlaps with $\delta^{13}C$ values of modern Arctic graminoids, shrubs, and aquatic mosses. Coupled with evidence for different sources of C_{22} and C_{28} *n*-alkanoic acid homologs in Units 1 and 3–5, we interpret the C_{22} *n*-alkanoic acid to be derived from aquatic plants and the C_{28} *n*-alkanoic acid to be from terrestrial higher plants. For Unit 2, we interpret all chain lengths to be from a terrestrial source and interpret only the C_{28} *n*-alkanoic acid. We discuss only the C_{22} and C_{28} *n*-alkanoic acids hereafter, due to sufficient abundance and distinct grouping with similar chain lengths.

We therefore interpret plant waxes at Camp Century to be derived from both aquatic and terrestrial plants, whereas brGDGTs at Camp Century appear to be dominated by lacustrine production. This difference likely reflects the distinct sources and production magnitudes of these biomarkers. Modern terrestrial and aquatic plants produce comparable concentration of waxes (Hollister et al., 2022), whereas brGDGT concentration is five-fold greater in modern lake sediments than soils (Martinez-Sosa et al., 2021; Guo et al., 2020) (Figure S10). This difference

https://doi.org/10.5194/egusphere-2026-2378
Preprint. Discussion started: 5 May 2026
© Author(s) 2026. CC BY 4.0 License.

in production magnitudes likely explains why the Camp Century brGDGTs appear dominated by lacustrine input, while the plant waxes reflect both environments.

3.1.2. Isotope Interpretation: The Mechanisms Influencing Source Water δ^2H values

Plant wax δ^2H values reflect the isotope value of the source water used by plants, with additional influence from evaporative enrichment of leaf water and biosynthetic fractionation (Sachse et al., 2012). Terrestrial plants use soil water, which primarily reflects summer precipitation δ^2H values, as most moisture inputs and active layer water recharge occur during the summer (Chiasson-Poirier et al., 2020; Gorbey et al., 2022; Thomas et al., 2020). However, the leaf water is typically more ^2H-enriched than the original source water, as evaporation preferentially removes isotopically lighter water molecules (Sachse et al., 2012). As a result, terrestrial plant waxes reflect summer precipitation δ^2H values plus evaporative ^2H-enrichment. On the other hand, aquatic plant wax δ^2H values reflect lake water δ^2H values as these plants take up water directly from their environment with little leaf water evaporative enrichment (Sachse et al., 2012). In Arctic lakes and streams, wax synthesis is greatest during the brief growing season when lakes are ice-free, so aquatic plant lipids predominantly record summer lake water δ^2H values. Since evaporation is limited, especially early during the ice-free season when leaf flush occurs (Akers et al., 2024; Cluett & Thomas, 2021; Tipple et al., 2013), lake water δ^2H that is uptaken by aquatic plants largely reflects summer precipitation δ^2H values. Accordingly, we interpret C_{22} δ^2H values to reflect summer precipitation δ^2H values and C_{28} δ^2H values to represent summer precipitation δ^2H values with evaporative ^2H-enrichment.

3.1.3. Climate Interpretation: The Mechanisms Influencing Precipitation δ^2H values

Precipitation isotope values integrate information about moisture source, transport history, and local condensation temperature (Dansgaard, 1964; Gimeno et al., 2021). We account for the impact of local condensation temperature using the independent brGDGT-inferred MAF

https://doi.org/10.5194/egusphere-2026-2378
Preprint. Discussion started: 5 May 2026
© Author(s) 2026. CC BY 4.0 License.

temperature and derive summer vapor δ^2H values (Section 2.1 and Text S3.7). Changes in vapor δ^2H values can therefore be interpreted to reflect changes in moisture source and transport history, without the effects of local condensation temperature. Relatively ^2H-enriched vapor tends to indicate shorter atmospheric moisture residence time, or more proximal transport pathways, while ^2H-depleted vapor occurs with longer atmospheric moisture residence time, due to more distal sources and greater distillation along the transport path (Cluett et al., 2018; Gat, 1996; Nusbaumer et al., 2017).

We interpret ^2H- and ^{18}O-enriched water vapor on Greenland to indicate proportionally more local- than remote-sourced moisture. Roughly 20% of modern summer moisture to Pittuffik is from land north of 60°N in North America, and another 10% from nearby marine sources: Baffin Bay and the Canadian Arctic Archipelago (Cluett et al., 2021). Moisture evapotranspired from these sources has a relatively short travel distance to northwestern Greenland, meaning the isotope value of moisture arriving at Pituffik from these sources is ^2H-enriched relative to the remaining 70% of moisture (Cluett et al., 2021; Gimeno et al., 2021). The remaining modern summer moisture to Pituffik is from remote sources in the Atlantic and Pacific Oceans and low-latitude landmasses, which deliver relatively ^2H-depleted moisture due to long transport times (Cluett et al., 2021). An increase in the proportion of locally-derived moisture to Greenland would cause vapor and resulting precipitation to be ^2H-enriched relative to modern (Cluett et al., 2021).

https://doi.org/10.5194/egusphere-2026-2378
Preprint. Discussion started: 5 May 2026
© Author(s) 2026. CC BY 4.0 License.

4. Results

4.1. Age, source, and inferred climate from molecular fossils in the Camp Century sedimentary units

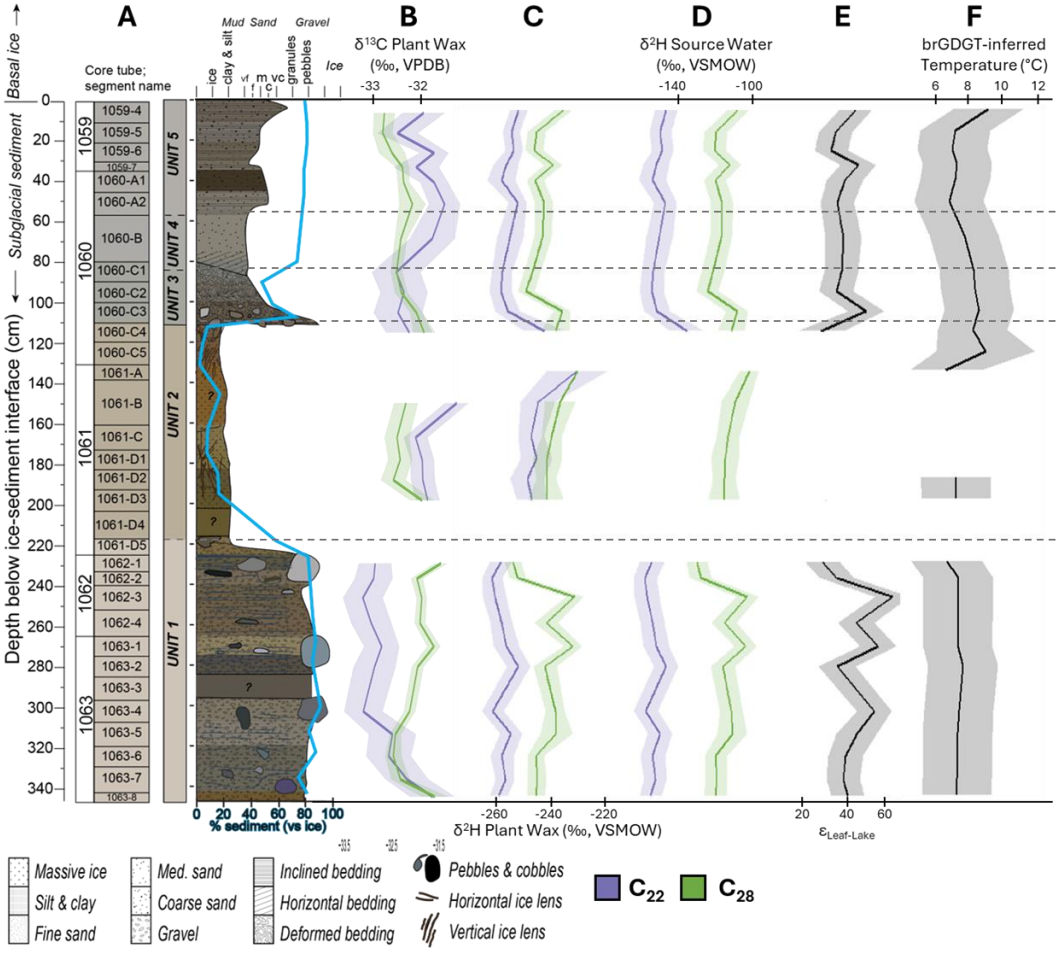

Figure 2. Biomarker data from Camp Century, Northwest Greenland. (A) Stratigraphic units and core log; blue line: percentage of sediment with respect to ice content (Bierman et al., 2024). (B) $\delta^{13}C$ of C_{22} and C_{28} *n*-alkanoic acids from Camp Century; (C) $\delta^{2}H$ of C_{22} and C_{28} *n*-alkanoic acids from Camp Century. (D) Plant-wax-inferred $\delta^{2}H$ value of lake and leaf water (E) calculated difference between leaf- and lake-water $\delta^{2}H$ values ($\varepsilon_{leaf\text{-}lake}$). (F) brGDGT-inferred temperature derived from two high-latitude lacustrine temperature calibrations (Otiniano et al., 2024; Raberg et al., 2021). Shading in B–E incorporates the standard error of the mean associated with the measured $\delta^{2}H$ and $\delta^{13}C$ values, which includes the uncertainty in the peak-size and drift

https://doi.org/10.5194/egusphere-2026-2378
Preprint. Discussion started: 5 May 2026
© Author(s) 2026. CC BY 4.0 License.

corrections, the replicate variability, and the methyl group correction. Shading in F represents the propagated standard error, incorporating the standard deviations of the reconstructed temperatures and the RMSEs of both calibrations.

Unit 1 in the Camp Century sub-ice material is characterized by poorly sorted, unstratified sediments with variable grain size and shape, consistent with basal till deposited subglacially as a single massive unit (Bierman et al., 2024b). The biomarkers preserved in this unit likely pre-date deposition, having been incorporated into the till from glacier-entrained soils, lakes, and vegetation present before glaciation. Given that Unit 1 was deposited >1.4 Mya (Christ et al., 2021), these biomarkers likely record climate conditions during the late Pliocene to early Pleistocene. brGDGT-inferred MAF temperatures ranged between 4.3 and 5.0°C (Figure 2F), with mean reconstructed values 4.1 ± 3.4°C above present-day conditions (Figure 3). The δ^2H value of lake water inferred from the C_{22} *n*-alkanoic acid ranged from -158 to -147 ‰, while in Unit 1 the δ^2H value of leaf water inferred from the C_{28} *n*-alkanoic acid ranged from -130 to -103 ‰ in Unit 1 (Figure 2D). Mean summer precipitation δ^2H values were 13 ± 14 ‰ ^2H-enriched relative to modern summer precipitation δ^2H values (Figure 4A). After accounting for the effect of local condensation temperature, summer atmospheric vapor was 19 ± 14 ‰ ^2H-enriched relative to the modern value (Figure 4B). Leaf water was 44 ± 9 ‰ ^2H-enriched relative to lake water (Equation S9, Figure 2E and 5B).

Unit 2 consists predominantly of ice with sparse dispersed sediments. This unit has not been directly dated but is most likely in stratigraphic order relative to Units 1 and 3 and therefore is between early-Pleistocene (Unit 1) and mid-Pleistocene (Unit 3) age. Biomarkers in Unit 2 may have been produced prior to deposition or could be roughly contemporaneous. brGDGT-inferred temperatures ranged from 4.8 to 6.6°C, with greater inter-sample variability than observed in the other units (Figure 2F). Mean MAF temperatures were 4.5 ± 3.1°C above modern conditions (Figure 3). We do not infer mean summer precipitation δ^2H values from Unit 2, as the wax distributions and isotope values indicate only terrestrial plant waxes are present in

https://doi.org/10.5194/egusphere-2026-2378
Preprint. Discussion started: 5 May 2026
© Author(s) 2026. CC BY 4.0 License.

this Unit. The δ^2H value of leaf water inferred from the C_{28} *n*-alkanoic acid ranged from -116 to -103 ‰ in Unit 2 (Figure 2D), which were slightly ^2H-enriched (5 ± 9 ‰) relative to the leaf water δ^2H values in the other four units but are within uncertainty (Equation S9, Figure 5A).

Units 3 through 5 contain well-sorted, finer-grained sediments with abundant plant macrofossils indicative of an ice-free environment (Bierman et al., 2024b; Collins et al., 2024). Deposited by low- to high-energy flowing water, these units likely represent deposition by summertime streams flowing across a periglacial landscape. The sediments appear to be in stratigraphic order and have been dated to approximately 416,000 ± 38,000 years ago (Christ et al., 2023; Woznick, 2024). Since the depositional environment was likely a subaerial stream surrounded by tundra (Christ et al., 2023), the preserved biomarkers were probably produced in this environment, roughly synchronous with sediment deposition. brGDGT-inferred MAF temperature ranged from 4.4 to 6.7 in Units 3 to 5. Mean brGDGT-inferred MAF temperature anomalies relative to modern were slightly higher in Unit 3 (5.2 ± 2.4°C) than in Units 4 (4.5 ± 1.8°C) and 5 (4.3 ± 2.9°C), although all are within uncertainty (Figure 3). The δ^2H value of lake water inferred from the C_{22} *n*-alkanoic acid ranged from -154 to -147 ‰ in Units 3 to 5, whereas the δ^2H value of leaf water inferred from the C_{28} *n*-alkanoic acid ranged from -125 to -109 ‰ in Units 3 to 5 (Figure 2D). Mean precipitation δ^2H values for the months above freezing were slightly ^2H-enriched, but within uncertainty of modern precipitation isotope values, with Unit 3 (14 ± 14 ‰) slightly ^2H-depleted relative to Units 4 and 5 (17 ± 14 ‰ and 17 ± 14 ‰, respectively) (Figure 4A). Summer atmospheric vapor δ^2H values were less strongly ^2H-enriched relative to modern vapor in Unit 3 (21 ± 14 ‰) than in Units 4 and 5 (22 ± 14 ‰ and 23± 14 ‰, respectively) (Figure 4B). Leaf water was ^2H-enriched relative to lake water, by a similar amount in all three units (~39 ± 9 ‰), similar to those values in unit 1 (Equation S9, Figure 2E and 5B).

https://doi.org/10.5194/egusphere-2026-2378
Preprint. Discussion started: 5 May 2026
© Author(s) 2026. CC BY 4.0 License.

4.2. Comparative Analysis of Greenland climate data

4.2.1. brGDGT temperature reconstructions

We compiled and analyzed (Section 2.3) eight published Holocene lacustrine brGDGT time series that form a latitudinal transect spanning southwestern Greenland (Figure 1): Lake 578 (61.080°N), Bullet Lake (63.982°N), Marshall Lake (64.464°N), Rosaea Lake (66.982°N), Lake Gus (67.032°N), Lake N3 (68.836°N), Pluto Lake (69.109°N), and Sikuiui Lake (70.218°N) (Acharya et al., 2025; Cluett et al., 2023; Schneider et al., 2024; Thomas et al., 2018). Using the same approach as we applied to the Camp Century samples, all eight of the Holocene brGDGT-inferred MAF temperatures are around 3 ± 2°C warmer than the modern observation, and about 2 to 3°C cooler than the anomaly reconstructed at Camp Century (Figure 3).

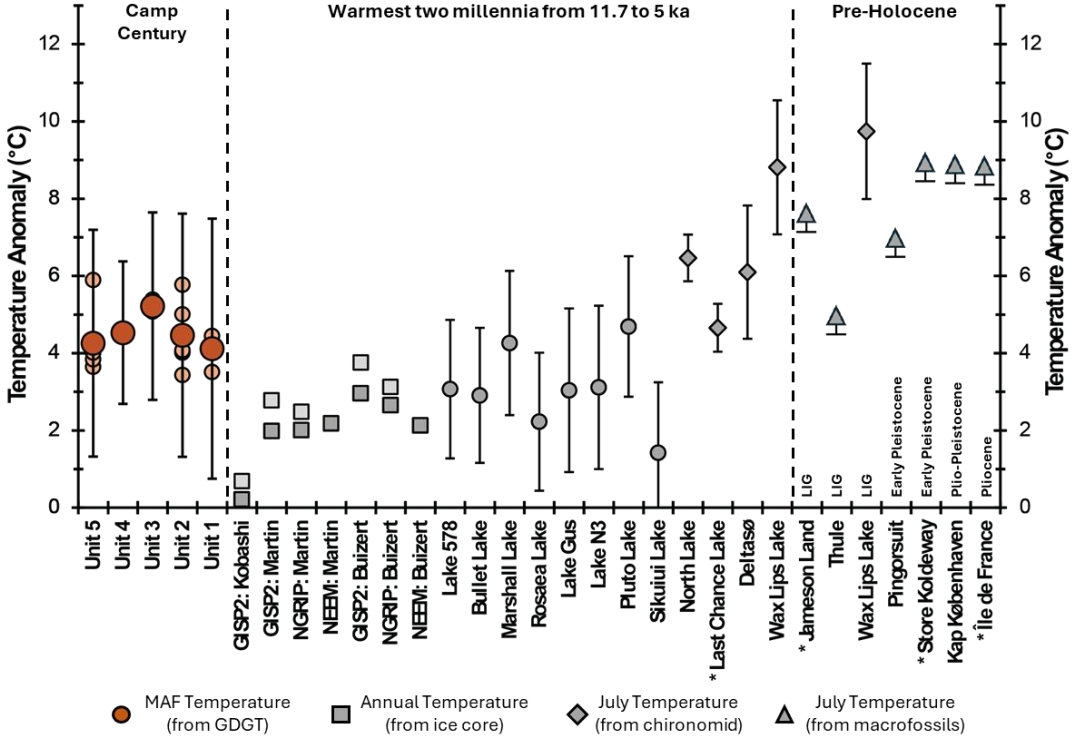

Figure 3. Air temperature anomaly relative to modern values (Table S1) for sites around Greenland. Sites marked with an asterisk (*) are located in eastern Greenland. Left: mean brGDGT-inferred temperature during the months above freezing (MAF) at Camp Century using

https://doi.org/10.5194/egusphere-2026-2378
Preprint. Discussion started: 5 May 2026
© Author(s) 2026. CC BY 4.0 License.

two high-latitude lacustrine calibrations (Raberg et al., 2021; Otiniano et al., 2024). Light orange circles: individual samples, dark orange circles: mean value for each Unit. Middle: Time series spanning the warmest two millenia from 11.7 to 5.0 ka, each proxy time arranged by latitude from south (left) to north (right). Right: Time series spanning pre-Holocene warm periods (LIG = Last Interglacial), each time period arranged by latitude from south (left) to north (right). Dark gray squares: mean annual air temperature inferred from argon and nitrogen isotopes from ice cores (Kobashi et al., 2017; Martin et al., 2024) and summer (JJA) temperatures inferred from ice core data assimilation (Buizert et al., 2018); Light gray squares: Elevation-corrected inferred temperatures, using elevations from Vinther et al. (2009); Gray circles: brGDGT-inferred MAF air temperature from Greenland lakes (Acharya et al., 2025; Cluett et al., 2023; Schneider et al., 2024; Thomas et al., 2018); gray diamonds: July air temperature inferred from chironomid assemblages using the Francis et al. (2006) calibration (Axford et al., 2019; Axford et al., 2017; Axford et al., 2013; McFarlin et al., 2018); vertical bars and arrow: July temperature inferred from plant macrofossils (Atti et al., 2024; Bennike, 1990; Bennike et al., 2002; Bennike & Böchner, 1992, 1994; Bennike et al., 2023; Bennike et al., 2010; Brodersen & Bennike, 2003; Hedenäs, 1994; Hedenäs & Bennike, 2003). Anomalies are calculated for the relevant seasonality of each proxy. Error bars incorporate propagated uncertainties (see methods). Error bars for ice core data are smaller than the symbol size.

To demonstrate the relative response of these time series independent of calibration choice, we also calculated the MBT'_{5Me} value for the Camp Century units and these eight Holocene time series (Figure S5). MBT'_{5Me} is an index incorporating temperature-sensitive brGDGTs (De Jonge et al., 2014), with a slope of 17.3 to 18.8 index value per °C in Arctic Lake sediments (Otiniano et al., 2024; Zhao et al., 2023). MBT'_{5Me} in Camp Century sedimentary brGDGTs is 0.23 – 0.31 MBT'_{5Me} units higher than the MBT'_{5Me} equivalent of the elevation-adjusted modern temperature at Camp Century (0.79°C) (Figure S5). MBT'_{5Me} values during the warmest two millennia from 11.7 to 5.0 ka at lakes 578 and Gus are ~0.1 MBT'_{5Me} units higher than the uppermost sample in the same cores, whereas at Lake N3, MBT'_{5Me} during this interval are comparable to those of the uppermost sample. Holocene MBT'_{5Me} across all southwestern Greenland lakes is 0.20 – 0.27 MBT'_{5Me} units higher than the MBT'_{5Me} equivalent of the modern MAF temperature at each site.

4.2.2. Chironomid and plant-based temperature reconstructions

There are three Holocene chironomid-inferred July temperature time series that span 69 to 76°N on western Greenland (Figure 1 and 3). These datasets suggest mean July temperature

https://doi.org/10.5194/egusphere-2026-2378
Preprint. Discussion started: 5 May 2026
© Author(s) 2026. CC BY 4.0 License.

during peak Holocene warmth was around 7.1 ± 2.9°C warmer than the modern observation (Axford et al., 2019; Axford et al., 2013; McFarlin et al., 2018), and approximately 2 to 4°C warmer than the temperature anomaly constructed at Camp Century (Figure 3).

Using the same analytical framework, pre-Holocene chironomid and plant macrofossils reconstructions provided direct comparison with the Camp Century record. Chironomid-inferred July temperature suggests the LIG on northwestern Greenland (76°N) was 9.7 ± 2.9°C warmer than modern July air temperature (McFarlin et al., 2018), and 5 to 6°C higher than the Camp Century MAF temperature anomalies (Figure 3). Plant macrofossil-based estimates provide minimum temperature constraints (and are therefore shown as arrows in Figure 3). During the LIG, Thule (northwestern Greenland) and Jameson Land (eastern Greenland) were at least 4.9°C and 7.5°C warmer than modern July air temperature, and at least 0.3°C and 3°C warmer than Camp Century MAF air temperatures, respectively (Bennike & Böchner, 1992, 1994; Broderson & Bennike, 2003; Hedenäs, 1994; Hedenäs & Bennike, 2003). Plant macrofossil- and insect-based estimates of Pliocene and Early Pleistocene July temperature at Pingorsuit (northwestern Greenland) and three sites in northeastern and northern Greenland have warmer temperature anomalies compared to those inferred at Camp Century (Atti et al., 2024; Bennike, 1990; Bennike et al., 2002; Bennike et al., 2010; Bennike et al., 2023).

5. Discussion

We infer that the biomarkers in MIS 11 sediments at Camp Century indicate MIS 11 conditions, given that they must have been produced in ice-free conditions at a site that is currently covered by 1387 m of ice and come from sediment layers interpreted as being deposited subaerially during the MIS 11 interglacial (Christ et al., 2021). Biomarkers preserved in the Unit 1 and 2 sediments have an unknown age but are likely from sometime in the Pliocene to mid-Pleistocene and were produced when the Camp Century site was ice free. Our

https://doi.org/10.5194/egusphere-2026-2378
Preprint. Discussion started: 5 May 2026
© Author(s) 2026. CC BY 4.0 License.

data indicate that MAF temperature and precipitation sources during interglacial periods in northwestern Greenland were broadly similar between MIS 11 and the other ice-free intervals recorded in Units 1 and 2. Compared to modern observations, summers were around 4.7°C warmer with a greater proportion of precipitation derived from local sources. These conditions are consistent with local ice-free conditions and the development of active terrestrial and aquatic ecosystems on an ice-free landscape. Comparison of the results with other Greenland paleoclimate records contributes to our understanding on the magnitude and spatial pattern of interglacial warmth across the ice sheet.

5.1. Northwestern Greenland climate: spatial and temporal comparison

5.1.1. Temperature

According to our brGDGT-based reconstruction, temperature of the months above freezing on northwestern Greenland was higher during MIS 11 than modern (Figure 3). To assess the magnitude of this warming in a broader context, we compare the Camp Century temperatures with other Greenland paleotemperature reconstructions that we compiled from multiple archives. We examine temperature estimates that are not based on water isotopes, as those can be additionally influenced by changes in the hydrological cycle (section 4.2.2.).

Camp Century brGDGT-derived temperatures are similar to or slightly higher than Holocene brGDGT-inferred temperature for southwestern Greenland, consistent with the slightly elevated MBT'_{5Me} values observed in the Camp Century sediments. The slightly higher temperature anomaly during past interglacials at Camp Century compared to the Holocene time series in southwestern Greenland may partly reflect polar amplification, rather than a similar magnitude of warming during the mid- and early Pleistocene and the Holocene. Comparison of Holocene temperature time series derived from the same proxies allows evaluation of polar amplification

https://doi.org/10.5194/egusphere-2026-2378
Preprint. Discussion started: 5 May 2026
© Author(s) 2026. CC BY 4.0 License.

while minimizing proxy-specific biases. There are no Holocene brGDGT-inferred temperature time series, however, at similar latitudes as the Camp Century site (Figure 1A and 3). The Holocene brGDGT time series spanning southwestern Greenland do not contain evidence for polar amplification of summer temperature, likely due to minimal sea ice cover in the nearby Labrador Sea and Baffin Bay and to a strong West Greenland Current that efficiently transported heat up the southwestern coast of Greenland (Acharya et al., 2025; Cluett et al., 2023; Gibb et al., 2015; Perner et al., 2013; Schneider et al., 2024). Mean-annual temperature inferred at ice-core sites contains evidence for later maximum Holocene temperature at more northern sites, but no difference in the magnitude of warming, even when corrected for elevation and seasonal effects (Figure 3) (Buizert, et al., 2018; Axford et al., 2021; Martin et al., 2024). Three Holocene chironomid-inferred July air temperature time series span 69 to 76°N on western Greenland (Figure 1 and 3), and contain equivocal evidence for polar amplification across this portion of Greenland. Two time series from northwestern Greenland have contrasting Holocene anomalies that are similar to and slightly greater than, but within uncertainty of, peak Holocene warmth in central western Greenland (Figure 3) (Axford et al., 2019; Axford et al., 2013; McFarlin et al., 2018).

Collectively, the available brGDGT-, chironomid-, and ice-core-inferred Holocene temperature data contain no strong evidence for polar amplification. If we assume that there was a similar lack of polar amplification across Greenland in pre-Holocene interglacial periods, then the fact that the mean Camp Century brGDGT-inferred MAF temperature anomaly is similar to the warmest two brGDGT-inferred Holocene millennia suggests that MIS11 summers were similar to peak warmth during the Holocene.

Comparing brGDGT-inferred MAF temperature at Camp Century to pre-Holocene temperature estimates elsewhere on Greenland provides a more comprehensive picture of how northwestern Greenland responded to past warmth (Figure 3). It is thought that the LIG period

https://doi.org/10.5194/egusphere-2026-2378
Preprint. Discussion started: 5 May 2026
© Author(s) 2026. CC BY 4.0 License.

was warmer than modern, yet ice-sheet models indicate a wide range of simulated ice sheet retreat during this period (Dahl-Jensen et al., 2013; Sommers et al., 2021). Temperature reconstructed using water isotopes from the NEEM ice core indicate that northern Greenland experienced temperatures substantially warmer than present during the LIG, with peak anomalies of several degrees above modern (Dahl-Jensen at al., 2013). On the other hand, the early Pleistocene and Pliocene climate and ice-sheet behavior are largely unconstrained. Chironomid and plant macrofossil-based temperature reconstructions indicate temperature anomalies during the LIG and Pliocene-Early Pleistocene that are comparable and slightly higher than those inferred at Camp Century (Atti et al., 2024; Axford et al., 2019; Axford et al., 2013; Bennike & Böchner, 1992, 1994; Bennike, 1990; Bennike et al., 2002; Bennike et al., 2010; Bennike et al., 2023; Broderson & Bennike, 2003; Hedenäs, 1994; Hedenäs & Bennike, 2003; McFarlin et al., 2018). However, these proxies differ in seasonal signal, as brGDGTs reflect MAF temperatures, whereas chironomid and plant macrofossil assemblages primarily reflect peak summer (particularly July) conditions, which tend to yield larger temperature anomalies. The smaller MAF temperature anomalies in Unit 1 of Camp Century relative to Early Pleistocene plant-based estimates therefore may reflect the difference in seasonal bias rather than reduced regional warmth. Together, these data indicate that the temperature during pre-Holocene interglacial periods in northern Greenland were similar to or slightly warmer than the Holocene.

Uncertainty in the age and origin of biomarkers of Unit 1 of Camp Century and other Early Pleistocene and Pliocene records on Greenland complicates direct comparison. It is possible that these samples were each deposited during a different interglacial or pre-glacial period within the Plio-Pleistocene, each characterized by distinct climatic conditions. The observed differences may reflect variability between separate interglacials rather than inconsistencies

https://doi.org/10.5194/egusphere-2026-2378
Preprint. Discussion started: 5 May 2026
© Author(s) 2026. CC BY 4.0 License.

among records of the same age. Even so, one key takeaway is that all proxies at all sites suggest temperatures higher than those of the late 20th century.

5.1.2. Water cycle

When the biomarkers in the Camp Century sediments were produced during MIS 11, the GrIS was much smaller than present, with at least 100 km more land between the west coast of Greenland and the ice-free Camp Century site. This ice-free land not only experienced temperatures above freezing (Figure 2F), but also supported plant biomass, as indicated by the presence of plants in the Camp Century sediments (Christ et al., 2021). Reduced snow and ice cover and greater plant biomass on Greenland and in high-latitude North America during Pleistocene interglacial periods would result in increased summer terrestrial evapotranspiration, which would cause a greater proportion of local moisture in northwestern Greenland.

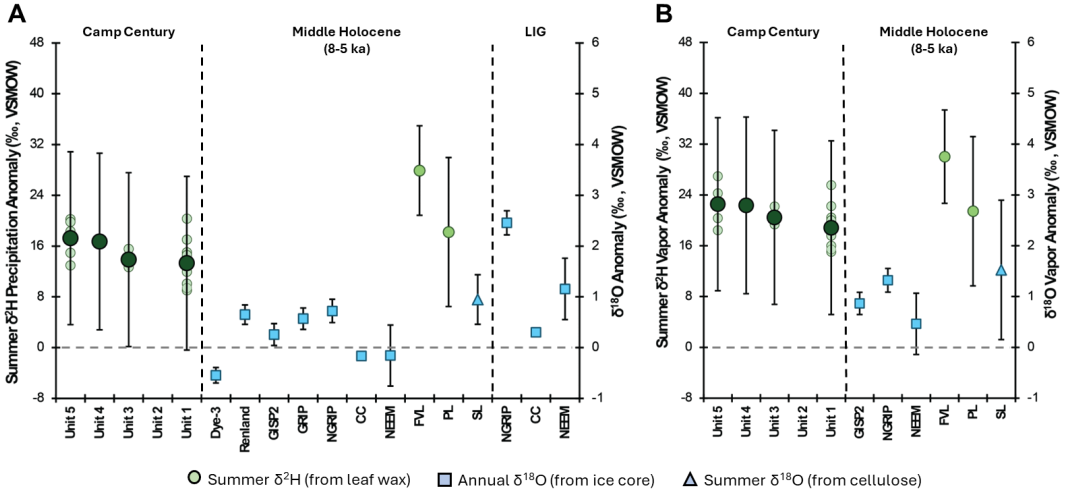

Figure 4. Water isotope anomaly relative to modern values (Table S2) for sites around Greenland. (A) Precipitation δ^2H anomaly (Bowen, 2017; Bowen et al., 2005; IAEA/WMO, 2015). Left: MAF precipitation δ^2H anomalies at Camp Century. Light green circles: individual samples, dark green circles: mean value for each unit. Middle: Middle Holocene (8 to 5 ka). Right: Last interglacial (LIG). (B) Summer vapor δ^2H or $\delta^{18}O$ anomalies derived using the local condensation temperature and precipitation isotope values for both modern (anomaly period)

https://doi.org/10.5194/egusphere-2026-2378
Preprint. Discussion started: 5 May 2026
© Author(s) 2026. CC BY 4.0 License.

and reconstructed precipitation isotope values (Clark & Fritz, 1997; Ellehoj et al., 2013; Majoube, 1971), using independent temperature reconstructions from the same or nearby archives (Acharya et al., 2025; Axford et al., 2017; Axford et al., 2019; Martin et al., 2024). Blue squares: mean annual precipitation $\delta^{18}O$ from ice cores (Andersen et al., 2004; Dahl-Jensen et al., 2013; Dansgaard et al., 1982; Dansgaard et al., 1969; Grootes & Stuiver, 1997; Johnsen et al., 1997; Schüpbach et al., 2018; Stuiver & Grootes, 2000; Vinther et al., 2009); Green circles: summer precipitation $\delta^{2}H$ inferred from leaf waxes (Balascio et al., 2013; Thomas et al., 2020); Blue triangle: summer precipitation $\delta^{18}O$ inferred from cellulose (Lasher et al., 2017). Error bars incorporate propagated uncertainties (see methods).

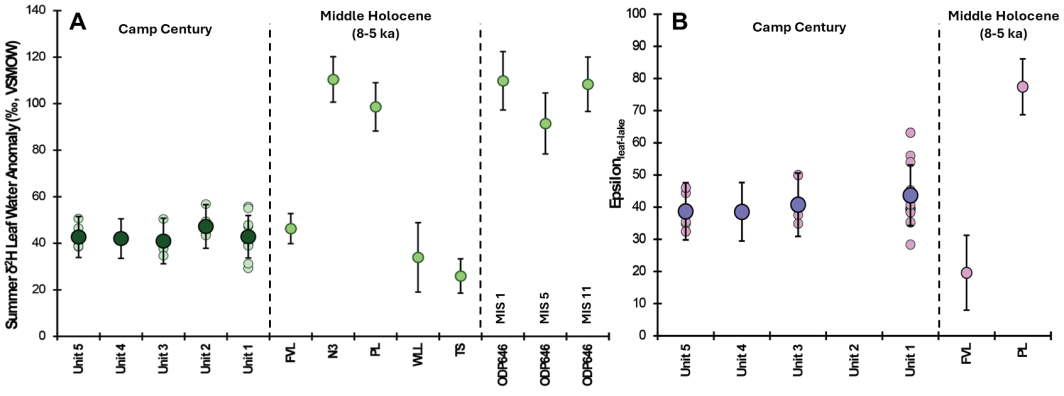

Figure 5. (A) Summer leaf water $\delta^{2}H$ anomaly, which reflects precipitation and evaporation, relative to mean modern summer $\delta^{2}H$ precipitation (Table S2) for sites around Greenland (Bowen, 2017; Bowen et al., 2005; IAEA/WMO, 2015). Left: summer leaf water $\delta^{2}H$ anomaly at Camp Century. Light green circles: individual samples, dark green circles: mean value for each unit. Middle: summer leaf water $\delta^{2}H$ anomalies for Greenland lake records spanning the middle Holocene (8 to 5 ka) (Balascio et al., 2013; McFarlin et al., 2023; Thomas et al., 2020). Right: summer leaf water $\delta^{2}H$ anomalies from SE Greenland records spanning Marine Isotope Stage (MIS) 1, 5 and 11 (Cluett & Thomas, 2021). (B) Left: Calculated isotope differences between inferred leaf water and lake water $\delta^{2}H$ in Camp Century compared to middle Holocene lake time series (right) (Balascio et al., 2013; Thomas et al., 2020). Pink circles: individual samples, violet circles, mean value for each unit. Error bars incorporate propagated uncertainties (see methods).

Our reconstructed summer water vapor isotope values at Camp Century were similar across all units, which have a mean value of 21 ± 19 ‰ ^{2}H-enriched relative to modern summer water vapor (Figure 4B). This is a larger anomaly than a Holocene $\delta^{18}O$ water vapor anomaly of 1.5 ± 1.4 ‰ (12 ± 11 ‰ when converted to $\delta^{2}H$ values using the Global Meteoric Water Line (GMWL)) at Secret Lake, near Pituffik, Greenland (Figure 4B) (Axford et al., 2019; Lasher et al., 2017;

https://doi.org/10.5194/egusphere-2026-2378
Preprint. Discussion started: 5 May 2026
© Author(s) 2026. CC BY 4.0 License.

Dansgaard, 1964). This indicates that in northwestern Greenland, summer vapor during MIS 11 (and during the periods recorded by Units 1 and 2) was ^{2}H-enriched compared to the Holocene, suggesting differences in moisture sourcing relative to Holocene conditions.

Holocene $\delta^{2}H$ vapor anomalies at Flower Valley Lake in southeastern Greenland and Pluto Lake in southwestern Greenland are 30 ± 7 ‰ and 21 ± 12 ‰, respectively (Figure 4B) (Balascio, et al., 2013; Thomas et al., 2020), indicating that southern Greenland experienced a comparable or slightly greater influence of locally derived moisture sources during the Holocene than did northwestern Greenland. Today, southwestern Greenland receives similar proportions of local and remote moisture as northwestern Greenland (Cluett et al., 2021), suggesting that these regional differences in moisture sourcing were likely amplified under warmer Holocene conditions. The high $\delta^{2}H$ values at the southern Greenland sites likely reflect greater evaporation from local seas and transpiration from terrestrial biomass during peak Holocene warmth, which would have contributed more ^{2}H-enriched moisture to vapor (Cluett et al., 2021). In contrast, relatively small Holocene $\delta^{18}O$ vapor anomalies at ice-core sites relative to Camp Century (Figure 4B) are likely because the ice cores reflect annual mean values, and are therefore influenced by strong seasonal changes in moisture source that do not impact the summer-biased isotope proxies (Buizert et al., 2018; Cluett et al., 2021; Kobashi et al., 2017; Martin et al., 2024; Nusbaumer et al., 2017; Sodemann et al., 2008).

This result aligns with evidence for both reduced GrIS extent (Reyes et al., 2014) and increased plant biomass in southern Greenland (de Vernal & Hillaire-Marcel, 2008) during MIS11 compared to both the Holocene and modern. Climate model simulations suggest that forest biomes may have expanded significantly northward in North America during MIS 11, replacing areas that were previously dominated by grasslands and tundra (Kleinen et al., 2014). Thus, ^{2}H-enriched vapor at Camp Century during the early and middle Pleistocene was likely

https://doi.org/10.5194/egusphere-2026-2378
Preprint. Discussion started: 5 May 2026
© Author(s) 2026. CC BY 4.0 License.

due to greater local evapotranspiration, consistent with reduced GrIS extent compared to both modern and to the period of peak Holocene warmth.

5.2. Summary and Climate Takeaway

MIS 11 summer temperature and moisture sources inferred from the Camp Century sediments complement existing terrestrial and marine temperature reconstructions from the North Atlantic Ocean and from terrestrial archives around Greenland. Because the Camp Century samples we analyzed were deposited at a location that is currently covered by 1387 m of ice, but must have been ice-free during their production, these biomarker-inferred temperature and water cycle data provide constraints on the sensitivity of the GrIS to climate forcing.

Based on the presence of, age constraints on, and abundance of biomarkers in the Camp Century sediments, we can infer that the Camp Century site was ice-free at least twice during the Plio/Pleistocene, once prior to the deposition of the till that forms Unit 1, and another time during MIS11 (Christ et al., 2021; Woznick, 2024). The climate inferred from the CC samples may not describe maximum interglacial conditions, as it is possible that portions of MIS11 are not preserved in the Camp Century stratigraphy, due to lack of deposition or subsequent erosion (Christ et al., 2021; Christ et al., 2023; Collins et al., 2025). For similar reasons, other interglacial periods, including MIS5 and early Pleistocene intervals, may have been ice-free at Camp Century but did not leave a sediment record. Nevertheless, the presence of plant fossils (Christ et al., 2021) and vapor isotope evidence for a greater contribution of local moisture to northwestern Greenland corroborates the inference of reduced ice-sheet extent during MIS 11 and an earlier interval.

These results shed new light on MIS 11 climate on Greenland. Similar summer temperature during the two intervals studied suggest interglacial temperature was relatively stable

https://doi.org/10.5194/egusphere-2026-2378
Preprint. Discussion started: 5 May 2026
© Author(s) 2026. CC BY 4.0 License.

throughout the Plio-Pleistocene, similar to previous findings (Herbert et al., 2010). During MIS 11, southeastern Greenland experienced moderate summer conditions similar to the Holocene, but that lasted on the order of 30,000 years, which in turn caused dramatic retreat of the southern portions of the GrIS (Cluett et al, 2021; Irvali et al., 2020; de Vernal & Hillaire-Marcel, 2008; Reyes et al., 2014). Available evidence from Camp Century suggests that northwestern Greenland also experienced MIS11 conditions similar to the Holocene. Therefore, like in southern Greenland, ice-sheet recession during MIS11 in northwestern Greenland may also have been caused by prolonged, rather than extreme, warmth, consistent with ice-sheet modeling showing that sustained moderate summer temperature anomalies over ~16,000 years can produce substantial GrIS mass loss (Robinson et al., 2017).

By 2100 CE, the Arctic will experience mean annual surface temperatures 3.0 to 10.6°C higher than 1950-2000 CE (Lee et al., 2023). The Camp Century brGDGT-inferred MAF temperature is at the low end of this range (Figure 3). Modern warming at high latitudes, however, is more pronounced in winter, which means that MAF temperatures will likely increase less than the predicted annual mean (Donohoe & Battisti, 2013; Dwyer et al., 2012). Cloud and albedo feedbacks, however, substantially increase GrIS sensitivity to warming under CMIP6 scenarios (Mostue et al., 2024). The Camp Century sub-ice sediments provide evidence that, due to sustained but moderate warmth during MIS11, the GrIS was >100 km behind its present margin, plants colonizing the ice-free land. The new temperature and water cycle constraints provided by biomarkers produced and deposited during MIS11 in Camp Century sub-ice sediments suggest that efforts to reduce both the magnitude and the duration of anthropogenic warmth will be important to restraining future GrIS retreat.

https://doi.org/10.5194/egusphere-2026-2378
Preprint. Discussion started: 5 May 2026
© Author(s) 2026. CC BY 4.0 License.

Acknowledgements

We thank the Kalaallit on whose territory Camp Century lies. The University at Buffalo operates on the territory of the Seneca Nation, a member of the Haudenosaunee/Six Nations Confederacy. We thank Owen Cowling, Nancy Leon and Jeff Salacup for laboratory assistance. This research was supported by NSF OPP 2114632 and a Fulbright Norway Scholar Award to EKT.

Conflict of Interest

Some authors are members of the editorial board of Climate of the Past for the special issue "The Camp Century ice and sediment core: new science from a 1966 core that touched the base of the Greenland ice sheet (CP/TC inter-journal SI)"

Data Availability Statement

Extracted samples are archived at the University at Buffalo. The raw lipid biomarker data generated and analyzed in this study are publicly available at the NOAA Paleoclimate Database (Aguilar et al., 2025).

References

Acharya, S., Cluett, A. A., Grogan, A. L., Briner, J. P., Castañeda, I. S., & Thomas, E. K. (2025). Holocene temperatures in southwestern Greenland controlled by topography, ice sheet proximity and oceanic conditions. *EGUsphere, 2025*, 1-32. https://egusphere.copernicus.org/preprints/2025/egusphere-2025-3113/

Aebly, F. A., & Fritz, S. C. (2009). Palaeohydrology of Kangerlussuaq (Søndre Strømfjord), West Greenland during the last ~8000 years. *The Holocene, 19*(1), 91-104. https://journals.sagepub.com/doi/abs/10.1177/0959683608096601

Aguilar, J. M. N., Thomas, E. K., Briner, J. P., Christ, A. J., Bierman, P. R., & Castañeda, I. S. (2025). NOAA/WDS Paleoclimatology—Camp Century Northwestern Greenland, Fatty

https://doi.org/10.5194/egusphere-2026-2378
Preprint. Discussion started: 5 May 2026
© Author(s) 2026. CC BY 4.0 License.

Acids and GDGTs, Early and Mid-Pleistocene [Data set]. NOAA National Centers for Environmental Information. https://doi.org/10.25921/8cqa-7a14

Akers, P. D., Kopec, B. G., Klein, E. S., Bailey, H., & Welker, J. M. (2024). The Pivotal Role of Evaporation in Lake Water Isotopic Variability Across Space and Time in a High Arctic Periglacial Landscape. *Water Resources Research, 60*(10), e2023WR036121. https://agupubs.onlinelibrary.wiley.com/doi/abs/10.1029/2023WR036121

Anderson, N. J., & Leng, M. J. (2004). Increased aridity during the early Holocene in West Greenland inferred from stable isotopes in laminated-lake sediments. *Quaternary Science Reviews, 23*(7), 841-849. https://www.sciencedirect.com/science/article/pii/S0277379104000113

Aschwanden, A., Fahnestock, M. A., Truffer, M., Brinkerhoff, D. J., Hock, R., Khroulev, C., et al. (2019). Contribution of the Greenland Ice Sheet to sea level over the next millennium. *Science Advances, 5*(6), eaav9396. https://www.science.org/doi/abs/10.1126/sciadv.aav9396

Atti, S., Bennike, O., & Weckström, K. (2024). Cladocerans and diatoms from an Early Pleistocene interglacial deposit at Pingorsuit, North-West Greenland. *Journal of Paleolimnology, 72*(3), 331-341. https://doi.org/10.1007/s10933-024-00333-z

Axford, Y., de Vernal, A., & Osterberg, E. C. (2021). Past Warmth and Its Impacts During the Holocene Thermal Maximum in Greenland. *Annual Review of Earth and Planetary Sciences, 49*(Volume 49, 2021), 279-307. https://www.annualreviews.org/content/journals/10.1146/annurev-earth-081420-063858

Axford, Y., Lasher, G. E., Kelly, M. A., Osterberg, E. C., Landis, J., Schellinger, G. C., et al. (2019). Holocene temperature history of northwest Greenland – With new ice cap constraints and chironomid assemblages from Deltasø. *Quaternary Science Reviews, 215*, 160-172. https://www.sciencedirect.com/science/article/pii/S0277379119302021

Axford, Y., Levy, L. B., Kelly, M. A., Francis, D. R., Hall, B. L., Langdon, P. G., & Lowell, T. V. (2017). Timing and magnitude of early to middle Holocene warming in East Greenland inferred from chironomids. *Boreas, 46*(4), 678-687. https://onlinelibrary.wiley.com/doi/abs/10.1111/bor.12247

Axford, Y., Losee, S., Briner, J. P., Francis, D. R., Langdon, P. G., & Walker, I. R. (2013). Holocene temperature history at the western Greenland Ice Sheet margin reconstructed from lake sediments. *Quaternary Science Reviews, 59*, 87-100. https://www.sciencedirect.com/science/article/pii/S0277379112004209

Balascio, N. L., D'Andrea, W. J., Bradley, R. S., & Perren, B. B. (2013). Biogeochemical evidence for hydrologic changes during the Holocene in a lake sediment record from southeast Greenland. *The Holocene, 23*(10), 1428-1439. https://doi.org/10.1177/0959683613493938

https://doi.org/10.5194/egusphere-2026-2378
Preprint. Discussion started: 5 May 2026
© Author(s) 2026. CC BY 4.0 License.

Bekryaev, R. V., Polyakov, I. V., & Alexeev, V. A. (2010). Role of Polar Amplification in Long-Term Surface Air Temperature Variations and Modern Arctic Warming. *Journal of Climate, 23*(14), 3888-3906. https://journals.ametsoc.org/view/journals/clim/23/14/2010jcli3297.1.xml

Bennike, O. (1990). The Kap København Formation: stratigraphy and palaeobotany of a Plio-Pleistocene sequence in Peary Land, North Greenland. *Meddelelser om Grønland. Geoscience, 23*, 85 pp. https://tidsskrift.dk/meddrgroenland_geosci/article/view/141978

Bennike, O., & Böcher, J. (1992). Early Weichselian interstadial land biotas at Thule, Northwest Greenland. *Boreas, 21*(2), 111-118. https://onlinelibrary.wiley.com/doi/abs/10.1111/j.1502-3885.1992.tb00019.x

Bennike, O., & Böcher, J. (1994). Land biotas of the last interglacial/glacial cycle on Jameson Land, East Greenland. *Boreas, 23*(4), 479-487. https://onlinelibrary.wiley.com/doi/abs/10.1111/j.1502-3885.1994.tb00615.x

Bennike, O., Abrahamsen, N., Bak, M., Israelson, C., Konradi, P., Matthiessen, J., & Witkowski, A. (2002). A multi-proxy study of Pliocene sediments from Île de France, North-East Greenland. *Palaeogeography, Palaeoclimatology, Palaeoecology, 186*(1), 1-23. https://www.sciencedirect.com/science/article/pii/S003101820200439X

Bennike, O., Knudsen, K. L., Abrahamsen, N., Bocher, J., Cremer, H., & Wagner, B. (2010). Early Pleistocene sediments on Store Koldewey, northeast Greenland. *Boreas, 39*(3), 603-619. https://onlinelibrary.wiley.com/doi/abs/10.1111/j.1502-3885.2010.00147.x

Bennike, O., Colgan, W., Hedenäs, L., Heiri, O., Lemdahl, G., Wiberg-Larsen, P., et al. (2023). An Early Pleistocene interglacial deposit at Pingorsuit, North-West Greenland. *Boreas, 52*(1), 27-41. https://onlinelibrary.wiley.com/doi/abs/10.1111/bor.12596

Bierman, P. R., Mastro, H. M., Peteet, D. M., Corbett, L. B., Steig, E. J., Halsted, C. T., et al. (2024a). Plant, insect, and fungi fossils under the center of Greenland's ice sheet are evidence of ice-free times. *Proceedings of the National Academy of Sciences, 121*(33), e2407465121. https://www.pnas.org/doi/abs/10.1073/pnas.2407465121

Bierman, P. R., Christ, A. J., Collins, C. M., Mastro, H. M., Souza, J., Blard, P. H., et al. (2024b). Scientific history, sampling approach, and physical characterization of the Camp Century sub-glacial sediment core, a rare archive from beneath the Greenland Ice Sheet. *EGUsphere, 2024*, 1-28. https://egusphere.copernicus.org/preprints/2024/egusphere-2023-2922/

Bowen, G. (2017). The Online Isotopes in Precipitation Calculator. Retrieved from http://www.waterisotopes.org

https://doi.org/10.5194/egusphere-2026-2378
Preprint. Discussion started: 5 May 2026
© Author(s) 2026. CC BY 4.0 License.

865 Bowen, G. J., Wassenaar, L. I., & Hobson, K. A. (2005). Global application of stable hydrogen
866 and oxygen isotopes to wildlife forensics. *Oecologia, 143*(3), 337-348.
867 https://doi.org/10.1007/s00442-004-1813-y

868 Box, J. E., Yang, L., Bromwich, D. H., & Bai, L.-S. (2009). Greenland Ice Sheet Surface Air
869 Temperature Variability: 1840–2007. *Journal of Climate, 22*(14), 4029-4049.
870 https://journals.ametsoc.org/view/journals/clim/22/14/2009jcli2816.1.xml

871 Brandes, C., Steffen, H., Steffen, R., Li, T., & Wu, P. (2025). Effects of the Last Quaternary
872 Glacial Forebulge on Vertical Land Movement, Sea-Level Change, and Lithospheric
873 Stresses. *Reviews of Geophysics, 63*(3), e2024RG000852.
874 https://agupubs.onlinelibrary.wiley.com/doi/abs/10.1029/2024RG000852

875 Briner, J. P., Stewart, H. A. M., Young, N. E., Philipps, W., & Losee, S. (2010). Using
876 proglacial-threshold lakes to constrain fluctuations of the Jakobshavn Isbræ ice margin,
877 western Greenland, during the Holocene. *Quaternary Science Reviews, 29*(27), 3861-
878 3874. https://www.sciencedirect.com/science/article/pii/S0277379110003276

879 Briner, J. P., Kaufman, D. S., Bennike, O., & Kosnik, M. A. (2014). Amino acid ratios in
880 reworked marine bivalve shells constrain Greenland Ice Sheet history during the
881 Holocene. *Geology, 42*(1), 75-78. https://doi.org/10.1130/G34843.1

882 Briner, J. P., McKay, N. P., Axford, Y., Bennike, O., Bradley, R. S., de Vernal, A., et al. (2016).
883 Holocene climate change in Arctic Canada and Greenland. *Quaternary Science*
884 *Reviews, 147*, 340-364.
885 https://www.sciencedirect.com/science/article/pii/S0277379116300427

886 Briner, J. P., & Bennike, O. (2025). An early Neoglacial moraine at Sanddalen, NE Greenland.
887 *Bulletin of the Geological Society of Denmark, 74*, 219-225.
888 https://doi.org/10.37570/bgsd-2025-74-12

889 Broderson, K. P., & Bennike, O. (2003). Interglacial Chironomidae (Diptera) from Thule,
890 Northwest Greenland: matching modern analogues to fossil assemblages. *Boreas,*
891 *32*(4), 560-565. https://onlinelibrary.wiley.com/doi/abs/10.1111/j.1502-
892 3885.2003.tb01235.x

893 Buizert, C., Keisling, B. A., Box, J. E., He, F., Carlson, A. E., Sinclair, G., & DeConto, R. M.
894 (2018). Greenland-Wide Seasonal Temperatures During the Last Deglaciation.
895 *Geophysical Research Letters, 45*(4), 1905-1914.
896 https://agupubs.onlinelibrary.wiley.com/doi/abs/10.1002/2017GL075601

897 Bullister, J. L., Rhein, M., & Mauritzen, C. (2013). Chapter 10 - Deepwater Formation. In G.
898 Siedler, S. M. Griffies, J. Gould, & J. A. Church (Eds.), *International Geophysics* (Vol.
899 103, pp. 227-253): Academic Press.

https://doi.org/10.5194/egusphere-2026-2378
Preprint. Discussion started: 5 May 2026
© Author(s) 2026. CC BY 4.0 License.

Callard, S. L., Ó Cofaigh, C., Lloyd, J. M., A. Smith, J., Gebhardt, C. A., Kanzow, T., & Roberts, D. H. (2025). Ocean driven retreat of the Northeast Greenland Ice Stream following the Last Glacial Maximum. *Nature Communications, 16*(1), 10961. https://doi.org/10.1038/s41467-025-66671-2

Caron, L., Ivins, E. R., Larour, E., Adhikari, S., Nilsson, J., & Blewitt, G. (2018). GIA Model Statistics for GRACE Hydrology, Cryosphere, and Ocean Science. *Geophysical Research Letters, 45*(5), 2203-2212. https://agupubs.onlinelibrary.wiley.com/doi/abs/10.1002/2017GL076644

Chiasson-Poirier, G., Franssen, J., Lafrenière, M. J., Fortier, D., & Lamoureux, S. F. (2020). Seasonal evolution of active layer thaw depth and hillslope-stream connectivity in a permafrost watershed. *Water Resources Research, 56*(1), e2019WR025828. https://agupubs.onlinelibrary.wiley.com/doi/abs/10.1029/2019WR025828

Christ, A. J., Bierman, P. R., Schaefer, J. M., Dahl-Jensen, D., Steffensen, J. P., Corbett, L. B., et al. (2021). A multimillion-year-old record of Greenland vegetation and glacial history preserved in sediment beneath 1.4 km of ice at Camp Century. *Proceedings of the National Academy of Sciences, 118*(13), e2021442118. https://doi.org/10.1073/pnas.2021442118

Christ, A. J., Rittenour, T. M., Bierman, P. R., Keisling, B. A., Knutz, P. C., Thomsen, T. B., et al. (2023). Deglaciation of northwestern Greenland during Marine Isotope Stage 11. *Science, 381*(6655), 330-335. https://www.science.org/doi/abs/10.1126/science.ade4248

Clark, I.D., & Fritz, P. (1997). Environmental Isotopes in Hydrogeology (1st ed.). CRC Press. https://doi.org/10.1201/9781482242911

Cluett, A. A., & Thomas, E. K. (2021). Summer warmth of the past six interglacials on Greenland. *Proceedings of the National Academy of Sciences, 118*(20), e2022916118. https://www.pnas.org/doi/abs/10.1073/pnas.2022916118

Cluett, A. A., Thomas, E. K., Evans, S. M., & Keys, P. W. . (2021). Seasonal Variations in Moisture Origin Explain Spatial Contrast in Precipitation Isotope Seasonality on Coastal Western Greenland. *Journal of Geophysical Research: Biogeosciences, 126*(11).

Cluett, A. A., Thomas, E. K., McKay, N. P., Cowling, O. C., Castañeda, I. S., & Morrill, C. (2023). Lake Dynamics Modulate the Air Temperature Variability Recorded by Sedimentary Aquatic Biomarkers: A Holocene Case Study From Western Greenland. *Journal of Geophysical Research: Biogeosciences, 128*(7), e2022JG007106. https://agupubs.onlinelibrary.wiley.com/doi/abs/10.1029/2022JG007106

Collins, C. M., Perdrial, N., Blard, P. H., Keulen, N., Mahaney, W. C., Mastro, H., et al. (2024). Characterization of the 1966 Camp Century Sub-Glacial Core: A Multiscale Analysis.

https://doi.org/10.5194/egusphere-2026-2378
Preprint. Discussion started: 5 May 2026
© Author(s) 2026. CC BY 4.0 License.

EGUsphere, 2024, 1-33. https://egusphere.copernicus.org/preprints/2024/egusphere-2024-2194/

Cronauer, S. L., Briner, J. P., Kelley, S. E., Zimmerman, S. R. H., & Morlighem, M. (2016). 10Be dating reveals early-middle Holocene age of the Drygalski Moraines in central West Greenland. *Quaternary Science Reviews, 147*, 59-68. https://www.sciencedirect.com/science/article/pii/S0277379115301050

Dahl-Jensen, D., Albert, M. R., Aldahan, A., Azuma, N., Balslev-Clausen, D., Baumgartner, M., et al. (2013). Eemian interglacial reconstructed from a Greenland folded ice core. *Nature, 493*(7433), 489-494. https://doi.org/10.1038/nature11789

Dansgaard, W. (1964). Stable isotopes in precipitation. *Tellus, 16*(4), 436-468. https://onlinelibrary.wiley.com/doi/abs/10.1111/j.2153-3490.1964.tb00181.x

de Vernal, A., & Hillaire-Marcel, C. (2008). Natural Variability of Greenland Climate, Vegetation, and Ice Volume During the Past Million Years. *Science, 320*(5883), 1622-1625. https://www.science.org/doi/abs/10.1126/science.1153929

Dion-Kirschner, H., McFarlin, J. M., Masterson, A. L., Axford, Y., & Osburn, M. R. (2020). Modern constraints on the sources and climate signals recorded by sedimentary plant waxes in west Greenland. *Geochimica et Cosmochimica Acta, 286*, 336-354. https://www.sciencedirect.com/science/article/pii/S0016703720304579

Donohoe, A., & Battisti, D. S. (2013). The Seasonal Cycle of Atmospheric Heating and Temperature. *Journal of Climate, 26*(14), 4962-4980. https://journals.ametsoc.org/view/journals/clim/26/14/jcli-d-12-00713.1.xml

Dwyer, J. G., Biasutti, M., & Sobel, A. H. (2012). Projected Changes in the Seasonal Cycle of Surface Temperature. *Journal of Climate, 25*(18), 6359-6374. https://journals.ametsoc.org/view/journals/clim/25/18/jcli-d-11-00741.1.xml

Ellehoj, M. D., Steen-Larsen, H. C., Johnsen, S. J., & Madsen, M. B. (2013). Ice-vapor equilibrium fractionation factor of hydrogen and oxygen isotopes: Experimental investigations and implications for stable water isotope studies. *Rapid Communications in Mass Spectrometry, 27*(19), 2149-2158. https://analyticalsciencejournals.onlinelibrary.wiley.com/doi/abs/10.1002/rcm.6668

Fausto, R. S., Ahlstrøm, A. P., Van As, D., Bøggild, C. E., & Johnsen, S. J. (2009). A new present-day temperature parameterization for Greenland. *Journal of Glaciology, 55*(189), 95-105. https://www.cambridge.org/core/product/A4C890F114971EF99BF0EF46140C8382

Francis, D. R., Wolfe, A. P., Walker, I. R., & Miller, G. H. (2006). Interglacial and Holocene temperature reconstructions based on midge remains in sediments of two lakes from Baffin Island, Nunavut, Arctic Canada. *Palaeogeography, Palaeoclimatology,*

https://doi.org/10.5194/egusphere-2026-2378
Preprint. Discussion started: 5 May 2026
© Author(s) 2026. CC BY 4.0 License.

Palaeoecology, 236(1), 107-124.
https://www.sciencedirect.com/science/article/pii/S0031018206000277

Fyke, J., Sergienko, O., Löfverström, M., Price, S., & Lenaerts, J. T. M. (2018). An Overview of Interactions and Feedbacks Between Ice Sheets and the Earth System. *Reviews of Geophysics, 56*(2), 361-408. https://agupubs.onlinelibrary.wiley.com/doi/abs/10.1029/2018RG000600

Gat, J. R. (1996). OXYGEN AND HYDROGEN ISOTOPES IN THE HYDROLOGIC CYCLE. *Annual Review of Earth and Planetary Sciences, 24*(Volume 24, 1996), 225-262. https://www.annualreviews.org/content/journals/10.1146/annurev.earth.24.1.225

Gibb, O. T., Steinhauer, S., Fréchette, B., de Vernal, A., & Hillaire-Marcel, C. (2015). Diachronous evolution of sea surface conditions in the Labrador Sea and Baffin Bay since the last deglaciation. *The Holocene, 25*(12), 1882-1897. https://journals.sagepub.com/doi/abs/10.1177/0959683615591352

Gimeno, L., Eiras-Barca, J., Durán-Quesada, A. M., Dominguez, F., van der Ent, R., Sodemann, H., et al. (2021). The residence time of water vapour in the atmosphere. *Nature Reviews Earth & Environment, 2*(8), 558-569. https://doi.org/10.1038/s43017-021-00181-9

Gorbey, D. B., Thomas, E. K., Sauer, P. E., Raynolds, M. K., Miller, G. H., Corcoran, M. C., et al. (2022). Modern Eastern Canadian Arctic Lake Water Isotopes Exhibit Latitudinal Patterns in Inflow Seasonality and Minimal Evaporative Enrichment. *Paleoceanography and Paleoclimatology, 37*(5), e2021PA004384. https://agupubs.onlinelibrary.wiley.com/doi/abs/10.1029/2021PA004384

Guo, J., Glendell, M., Meersmans, J., Kirkels, F., Middelburg, J. J., & Peterse, F. (2020). Assessing branched tetraether lipids as tracers of soil organic carbon transport through the Carminowe Creek catchment (southwest England). *Biogeosciences, 17*(12), 3183-3201. https://bg.copernicus.org/articles/17/3183/2020/

Guo, X., Zhao, L., Gladstone, R. M., Sun, S., & Moore, J. C. (2019). Simulated retreat of Jakobshavn Isbræ during the 21st century. *The Cryosphere, 13*(11), 3139-3153. https://tc.copernicus.org/articles/13/3139/2019/

Harning, D. J., Sacco, S., Raberg, J. H., Ardenghi, N., Sepúlveda, J., Shapiro, B., et al. (2025). Both redox potential and climate control molecular proxies in Icelandic Holocene lake sediments. *Communications Earth & Environment, 6*(1), 763. https://doi.org/10.1038/s43247-025-02701-7

Hatfield, R. G., Reyes, A. V., Stoner, J. S., Carlson, A. E., Beard, B. L., Winsor, K., & Welke, B. (2016). Interglacial responses of the southern Greenland ice sheet over the last 430,000 years determined using particle-size specific magnetic and isotopic tracers.

https://doi.org/10.5194/egusphere-2026-2378
Preprint. Discussion started: 5 May 2026
© Author(s) 2026. CC BY 4.0 License.

Earth and Planetary Science Letters, 454, 225-236. https://www.sciencedirect.com/science/article/pii/S0012821X16304940

Hedenäs, L. (1994). Bryophytes from the last interglacial/glacial cycle, Jameson Land, East Greenland. *Boreas, 23*(4), 488-494. https://onlinelibrary.wiley.com/doi/abs/10.1111/j.1502-3885.1994.tb00616.x

Hedenäs, L., & Bennike, O. (2003). Moss Remains from the Last Interglacial at Thule, NW Greenland. *Lindbergia, 28*(2), 52-58. http://www.jstor.org/stable/20150125

Herbert, T. D., Peterson, L. C., Lawrence, K. T., & Liu, Z. (2010). Tropical Ocean Temperatures Over the Past 3.5 Million Years. *Science, 328*(5985), 1530-1534. https://www.science.org/doi/abs/10.1126/science.1185435

Hersbach, H., Bell, B., Berrisford, P., Hirahara, S., Horányi, A., Muñoz-Sabater, J., et al. (2020). The ERA5 global reanalysis. *Quarterly Journal of the Royal Meteorological Society, 146*(730), 1999-2049. https://rmets.onlinelibrary.wiley.com/doi/abs/10.1002/qj.3803

Holland, D. M., Thomas, R. H., de Young, B., Ribergaard, M. H., & Lyberth, B. (2008). Acceleration of Jakobshavn Isbræ triggered by warm subsurface ocean waters. *Nature Geoscience, 1*(10), 659-664. https://doi.org/10.1038/ngeo316

Hollister, K. V., Thomas, E. K., Raynolds, M. K., Bültmann, H., Raberg, J. H., Miller, G. H., & Sepúlveda, J. (2022). Aquatic and Terrestrial Plant Contributions to Sedimentary Plant Waxes in a Modern Arctic Lake Setting. *Journal of Geophysical Research: Biogeosciences, 127*(8), e2022JG006903. https://agupubs.onlinelibrary.wiley.com/doi/abs/10.1029/2022JG006903

Holtzman, H., Thomas, E. K., Erb, M., Marshall, L., Castañeda, I. S., Kaufman, D., et al. (2025). Early Holocene Atmospheric Circulation Changes Over Northern Europe Based on Isotopic and Biomarker Evidence From Kola Peninsula. *Paleoceanography and Paleoclimatology, 40*(3), e2024PA005076. https://agupubs.onlinelibrary.wiley.com/doi/abs/10.1029/2024PA005076

IAEA/WMO, Global Network of Isotopes in Precipitation, GNIP Database [data set], https://nucleus.iaea.org/wiser, 2015.

Irvalı, N., Galaasen, E. V., Ninnemann, U. S., Rosenthal, Y., Born, A., & Kleiven, H. F. (2020). A low climate threshold for south Greenland Ice Sheet demise during the Late Pleistocene. *Proceedings of the National Academy of Sciences, 117*(1), 190-195. https://www.pnas.org/doi/abs/10.1073/pnas.1911902116

Jansen, E., Fronval, T., Rack, F., & Channell, J. E. T. (2000). Pliocene-Pleistocene ice rafting history and cyclicity in the Nordic Seas during the last 3.5 Myr. *Paleoceanography, 15*(6), 709-721. https://agupubs.onlinelibrary.wiley.com/doi/abs/10.1029/1999PA000435

https://doi.org/10.5194/egusphere-2026-2378
Preprint. Discussion started: 5 May 2026
© Author(s) 2026. CC BY 4.0 License.

Jensen, C. D. (2025). *Weather Observations from Greenland 1958-2024*. Retrieved from https://www.dmi.dk/fileadmin/Rapporter/2025/DMIRep25-08.pdf

John, K. E. K. S., & Krissek, L. A. (2002). The late Miocene to Pleistocene ice-rafting history of southeast Greenland. *Boreas, 31*(1), 28-35. https://onlinelibrary.wiley.com/doi/abs/10.1111/j.1502-3885.2002.tb01053.x

Kleinen, T., Hildebrandt, S., Prange, M., Rachmayani, R., Müller, S., Bezrukova, E., et al. (2014). The climate and vegetation of Marine Isotope Stage 11 – Model results and proxy-based reconstructions at global and regional scale. *Quaternary International, 348*, 247-265. https://www.sciencedirect.com/science/article/pii/S1040618213009622

Kobashi, T., Menviel, L., Jeltsch-Thömmes, A., Vinther, B. M., Box, J. E., Muscheler, R., et al. (2017). Volcanic influence on centennial to millennial Holocene Greenland temperature change. *Scientific Reports, 7*(1), 1441. https://doi.org/10.1038/s41598-017-01451-7

Koerner, R., & Russell, R. D. (1979). δ18O variations in snow on the Devon Island ice cap, Northwest Territories, Canada. *Canadian Journal of Earth Sciences, 16*(7), 1419-1427. https://cdnsciencepub.com/doi/abs/10.1139/e79-126

Konecky, B. L., McKay, N. P., Churakova, O. V., Comas-Bru, L., Dassié, E. P., DeLong, K. L., et al. (2020). The Iso2k database: a global compilation of paleo-δ18O and δ2H records to aid understanding of Common Era climate. *Earth Syst. Sci. Data, 12*(3), 2261-2288. https://essd.copernicus.org/articles/12/2261/2020/

Larsen, N. K., Kjær, K. H., Lecavalier, B., Bjørk, A. A., Colding, S., Huybrechts, P., et al. (2015). The response of the southern Greenland ice sheet to the Holocene thermal maximum. *Geology, 43*(4), 291-294. https://doi.org/10.1130/G36476.1

Larsen, H. C., Saunders, A. D., Clift, P. D., Beget, J., Wei, W., & Spezzaferri, S. (1994). Seven Million Years of Glaciation in Greenland. *Science, 264*(5161), 952-955. https://www.science.org/doi/abs/10.1126/science.264.5161.952

Lasher, G. E., Axford, Y., McFarlin, J. M., Kelly, M. A., Osterberg, E. C., & Berkelhammer, M. B. (2017). Holocene temperatures and isotopes of precipitation in Northwest Greenland recorded in lacustrine organic materials. *Quaternary Science Reviews, 170*, 45-55. https://www.sciencedirect.com/science/article/pii/S0277379116305650

Lawrence, K. T., Herbert, T. D., Brown, C. M., Raymo, M. E., & Haywood, A. M. (2009). High-amplitude variations in North Atlantic sea surface temperature during the early Pliocene warm period. *Paleoceanography, 24*(2). https://agupubs.onlinelibrary.wiley.com/doi/abs/10.1029/2008PA001669

Lawrence, K. T., Sosdian, S., White, H. E., & Rosenthal, Y. (2010). North Atlantic climate evolution through the Plio-Pleistocene climate transitions. *Earth and Planetary Science*

https://doi.org/10.5194/egusphere-2026-2378
Preprint. Discussion started: 5 May 2026
© Author(s) 2026. CC BY 4.0 License.

Letters, 300(3), 329-342. https://www.sciencedirect.com/science/article/pii/S0012821X10006473

Lecavalier, B. S., Milne, G. A., Simpson, M. J. R., Wake, L., Huybrechts, P., Tarasov, L., et al. (2014). A model of Greenland ice sheet deglaciation constrained by observations of relative sea level and ice extent. *Quaternary Science Reviews, 102*, 54-84. https://www.sciencedirect.com/science/article/pii/S0277379114003011

Lee, J.-Y. M., J.; Bala, G.; Cao, L.; Corti, S.; Dunne, J.P.; Engelbrecht, F.; Fischer, E.; Fyfe, J.C.; Jones, C.; Maycock, A.; Mutemi, J.; Ndiaye, O.; Panickal, S.; Zhou, T. (2023). Future Global Climate: Scenario-based Projections and Near-term Information. In V. Z. Masson-Delmotte, P.; Pirani, A.; Connors, S.L.; Péan, C.; Berger, S.; Caud, N.; Chen, Y.; Goldfarb, L.; Gomis, M.I.; Huang, M.; Leitzell, K.; Lonnoy, E.; Matthews, J.B.R.; Maycock, T.K.; Waterfield, T.; Yelekçi, O.; Yu, R.; Zhou, B. (Ed.), *Climate Change 2021 – The Physical Science Basis: Working Group I Contribution to the Sixth Assessment Report of the Intergovernmental Panel on Climate Change* (pp. 553-672). Cambridge: Cambridge University Press.

Lindberg, K. R., Daniels, W. C., Castañeda, I. S., & Brigham-Grette, J. (2022). Biomarker proxy records of Arctic climate change during the Mid-Pleistocene transition from Lake El'gygytgyn (Far East Russia). *Clim. Past, 18*(3), 559-577. https://cp.copernicus.org/articles/18/559/2022/

Majoube, M. (1971). Fractionnement en oxygène 18 et en deutérium entre l'eau et sa vapeur. *J. Chim. Phys., 68*, 1423-1436. https://doi.org/10.1051/jcp/1971681423

Martin, K. C., Buizert, C., Brook, E., Williams, O. L., Edwards, J. S., Riddell-Young, B., et al. (2024). Greenland Ice Cores Reveal a South-To-North Difference in Holocene Thermal Maximum Timings. *Geophysical Research Letters, 51*(24), e2024GL111405. https://agupubs.onlinelibrary.wiley.com/doi/abs/10.1029/2024GL111405

Martínez-Sosa, P., Tierney, J. E., Stefanescu, I. C., Dearing Crampton-Flood, E., Shuman, B. N., & Routson, C. (2021). A global Bayesian temperature calibration for lacustrine brGDGTs. *Geochimica et Cosmochimica Acta, 305*, 87-105. https://www.sciencedirect.com/science/article/pii/S0016703721002635

Martínez-Sosa, P., Tierney, J. E., Pérez-Angel, L. C., Stefanescu, I. C., Guo, J., Kirkels, F., et al. (2023). Development and Application of the Branched and Isoprenoid GDGT Machine Learning Classification Algorithm (BIGMaC) for Paleoenvironmental Reconstruction. *Paleoceanography and Paleoclimatology, 38*(7), e2023PA004611. https://agupubs.onlinelibrary.wiley.com/doi/abs/10.1029/2023PA004611

McFarlin, J. M., Axford, Y., Osburn, M. R., Kelly, M. A., Osterberg, E. C., & Farnsworth, L. B. (2018). Pronounced summer warming in northwest Greenland during the Holocene and Last Interglacial. *Proceedings of the National Academy of Sciences, 115*(25), 6357-6362. https://www.pnas.org/doi/abs/10.1073/pnas.1720420115

https://doi.org/10.5194/egusphere-2026-2378
Preprint. Discussion started: 5 May 2026
© Author(s) 2026. CC BY 4.0 License.

Melles, M., Brigham-Grette, J., Minyuk, P. S., Nowaczyk, N. R., Wennrich, V., DeConto, R. M., et al. (2012). 2.8 Million Years of Arctic Climate Change from Lake El'gygytgyn, NE Russia. *Science, 337*(6092), 315-320. https://www.science.org/doi/abs/10.1126/science.1222135

Miller, G. H., Alley, R. B., Brigham-Grette, J., Fitzpatrick, J. J., Polyak, L., Serreze, M. C., & White, J. W. C. (2010). Arctic amplification: can the past constrain the future? *Quaternary Science Reviews, 29*(15), 1779-1790. https://www.sciencedirect.com/science/article/pii/S0277379110000405

Morlighem, M., Williams, C. N., Rignot, E., An, L., Arndt, J. E., Bamber, J. L., et al. (2017). BedMachine v3: Complete Bed Topography and Ocean Bathymetry Mapping of Greenland From Multibeam Echo Sounding Combined With Mass Conservation. *Geophysical Research Letters, 44*(21), 11,051-011,061. https://agupubs.onlinelibrary.wiley.com/doi/abs/10.1002/2017GL074954

Mostue, I. A., Hofer, S., Storelvmo, T., & Fettweis, X. (2024). Cloud- and ice-albedo feedbacks drive greater Greenland Ice Sheet sensitivity to warming in CMIP6 than in CMIP5. *The Cryosphere, 18*(1), 475-488. https://tc.copernicus.org/articles/18/475/2024/

Naafs, B. D. A., Inglis, G. N., Zheng, Y., Amesbury, M. J., Biester, H., Bindler, R., et al. (2017). Introducing global peat-specific temperature and pH calibrations based on brGDGT bacterial lipids. *Geochimica et Cosmochimica Acta, 208*, 285-301. https://www.sciencedirect.com/science/article/pii/S0016703717300522

Nowicki, S. M. J., Payne, A., Larour, E., Seroussi, H., Goelzer, H., Lipscomb, W., et al. (2016). Ice Sheet Model Intercomparison Project (ISMIP6) contribution to CMIP6. *Geosci. Model Dev., 9*(12), 4521-4545. https://gmd.copernicus.org/articles/9/4521/2016/

Nusbaumer, J., Wong, T. E., Bardeen, C., & Noone, D. (2017). Evaluating hydrological processes in the Community Atmosphere Model Version 5 (CAM5) using stable isotope ratios of water. *Journal of Advances in Modeling Earth Systems, 9*(2), 949-977. https://agupubs.onlinelibrary.wiley.com/doi/abs/10.1002/2016MS000839

O'Connor, K. F., Berke, M. A., & Ziolkowski, L. A. (2020). Hydrogen isotope fractionation in modern plants along a boreal-tundra transect in Alaska. *Organic Geochemistry, 147*, 104064. https://www.sciencedirect.com/science/article/pii/S0146638020300991

Otiniano, G. A., Porter, T. J., Phillips, M. A., Juutinen, S., Weckström, J. B., & Heikkilä, M. P. (2024). Reconstructing warm-season temperatures using brGDGTs and assessing biases in Holocene temperature records in northern Fennoscandia. *Quaternary Science Reviews, 329*, 108555. https://www.sciencedirect.com/science/article/pii/S0277379124000568

https://doi.org/10.5194/egusphere-2026-2378
Preprint. Discussion started: 5 May 2026
© Author(s) 2026. CC BY 4.0 License.

Paxman, G. J. G., Austermann, J., & Hollyday, A. (2022). Total isostatic response to the complete unloading of the Greenland and Antarctic Ice Sheets. *Scientific Reports, 12*(1), 11399. https://doi.org/10.1038/s41598-022-15440-y

Perner, K., Moros, M., Jennings, A., Lloyd, J., & Knudsen, K. (2013). Holocene palaeoceanographic evolution off West Greenland. *The Holocene, 23*(3), 374-387. https://journals.sagepub.com/doi/abs/10.1177/0959683612460785

Raberg, J. H., Harning, D. J., Crump, S. E., de Wet, G., Blumm, A., Kopf, S., et al. (2021). Revised fractional abundances and warm-season temperatures substantially improve brGDGT calibrations in lake sediments. *Biogeosciences, 18*(12), 3579-3603. https://bg.copernicus.org/articles/18/3579/2021/

Raberg, J. H., de Wet, G. A., Geirsdóttir, Á., Sepúlveda, J., & Miller, G. H. (2025). Oxygen Depletion in Lake Waters May Skew brGDGT-Inferred Temperatures by More Than 10°C. *Geophysical Research Letters, 52*(15), e2024GL113562. https://agupubs.onlinelibrary.wiley.com/doi/abs/10.1029/2024GL113562

Raymo, M., Ruddiman, W. F., & Clement, B. (1987). Pliocene-Pleistocene Paleoceanography of the North Atlantic at Deep Sea Drilling Project Site 609. *Initial reports DSDP, Leg 94, Norfolk, Virginia to St. John's, Newfoundland. Part 2, 94*, 895-901.

Raymo, M. E., Ruddiman, W. F., Backman, J., Clement, B. M., & Martinson, D. G. (1989). Late Pliocene variation in northern hemisphere ice sheets and North Atlantic deep water circulation. *Paleoceanography, 4*(4), 413-446. https://agupubs.onlinelibrary.wiley.com/doi/abs/10.1029/PA004i004p00413

Reyes, A. V., Carlson, A. E., Beard, B. L., Hatfield, R. G., Stoner, J. S., Winsor, K., et al. (2014). South Greenland ice-sheet collapse during Marine Isotope Stage 11. *Nature, 510*(7506), 525-528.

Robinson, A., Alvarez-Solas, J., Calov, R., Ganopolski, A., & Montoya, M. (2017). MIS-11 duration key to disappearance of the Greenland ice sheet. *Nature Communications, 8*(1), 16008. https://doi.org/10.1038/ncomms16008

Russell, J. M., Hopmans, E. C., Loomis, S. E., Liang, J., & Sinninghe Damsté, J. S. (2018). Distributions of 5- and 6-methyl branched glycerol dialkyl glycerol tetraethers (brGDGTs) in East African lake sediment: Effects of temperature, pH, and new lacustrine paleotemperature calibrations. *Organic Geochemistry, 117*, 56-69. https://www.sciencedirect.com/science/article/pii/S0146638017304394

Sachse, D., Isabelle, B., Bowen, G., Chikaraishi, Y., Dawson, T., Feakins, S., et al. (2012). Molecular Paleohydrology: Interpreting the Hydrogen-Isotopic Composition of Lipid Biomarkers from Photosynthesizing Organisms. *Annual Review of Earth and Planetary Sciences, 40*, 221-249.

https://doi.org/10.5194/egusphere-2026-2378
Preprint. Discussion started: 5 May 2026
© Author(s) 2026. CC BY 4.0 License.

Schaefer, J. M., Finkel, R. C., Balco, G., Alley, R. B., Caffee, M. W., Briner, J. P., et al. (2016). Greenland was nearly ice-free for extended periods during the Pleistocene. *Nature, 540*(7632), 252-255. https://doi.org/10.1038/nature20146

Schneider, T., Castañeda, I. S., Zhao, B., Krüger, S., Salacup, J. M., & Bradley, R. S. (2024). Tracing Holocene temperatures and human impact in a Greenlandic Lake: Novel insights from hyperspectral imaging and lipid biomarkers. *Quaternary Science Reviews, 339*, 108851. https://www.sciencedirect.com/science/article/pii/S0277379124003524

Shackleton, N. J., Backman, J., Zimmerman, H., Kent, D. V., Hall, M. A., Roberts, D. G., et al. (1984). Oxygen isotope calibration of the onset of ice-rafting and history of glaciation in the North Atlantic region. *Nature, 307*(5952), 620-623. https://doi.org/10.1038/307620a0

Sinninghe Damsté, J. S., Hopmans, E. C., Pancost, R. D., Schouten, S., & Geenevasen, J. A. J. (2000). Newly discovered non-isoprenoid glycerol dialkyl glycerol tetraether lipids in sediments. *Chemical Communications*(17), 1683-1684. 10.1039/B004517I. http://dx.doi.org/10.1039/B004517I

Sinninghe Damsté, J. S., Schouten, S., Hopmans, E. C., van Duin, A. C. T., & Geenevasen, J. A. J. (2002). Crenarchaeol. *Journal of Lipid Research, 43*(10), 1641-1651. https://www.sciencedirect.com/science/article/pii/S0022227520327838

Smith, B., Fricker, H. A., Gardner, A. S., Medley, B., Nilsson, J., Paolo, F. S., et al. (2020). Pervasive ice sheet mass loss reflects competing ocean and atmosphere processes. *Science, 368*(6496), 1239-1242. https://www.science.org/doi/abs/10.1126/science.aaz5845

Sodemann, H., Masson-Delmotte, V., Schwierz, C., Vinther, B. M., & Wernli, H. (2008). Interannual variability of Greenland winter precipitation sources: 2. Effects of North Atlantic Oscillation variability on stable isotopes in precipitation. *Journal of Geophysical Research: Atmospheres, 113*(D12). https://agupubs.onlinelibrary.wiley.com/doi/abs/10.1029/2007JD009416

Sommers, A. N., Otto-Bliesner, B. L., Lipscomb, W. H., Lofverstrom, M., Shafer, S. L., Bartlein, P. J., et al. (2021). Retreat and Regrowth of the Greenland Ice Sheet During the Last Interglacial as Simulated by the CESM2-CISM2 Coupled Climate–Ice Sheet Model. *Paleoceanography and Paleoclimatology, 36*(12), e2021PA004272. https://agupubs.onlinelibrary.wiley.com/doi/abs/10.1029/2021PA004272

St. John, K. E. K., & Krissek, L. A. (2002). The late Miocene to Pleistocene ice-rafting history of southeast Greenland. *Boreas, 31*(1), 28-35. https://onlinelibrary.wiley.com/doi/abs/10.1111/j.1502-3885.2002.tb01053.x

Tabone, I., Robinson, A., Montoya, M., & Alvarez-Solas, J. (2024). Holocene thinning in central Greenland controlled by the Northeast Greenland Ice Stream. *Nature Communications, 15*(1), 6434. https://doi.org/10.1038/s41467-024-50772-5

https://doi.org/10.5194/egusphere-2026-2378
Preprint. Discussion started: 5 May 2026
© Author(s) 2026. CC BY 4.0 License.

Tipple, B. J., Berke, M. A., Doman, C. E., Khachaturyan, S., & Ehleringer, J. R. (2013). Leaf-wax *n*-alkanes record the plant-water environment at leaf flush. *Proceedings of the National Academy of Sciences, 110*(7), 2659-2664. https://www.pnas.org/doi/abs/10.1073/pnas.1213875110

Thomas, E., Briner, J., Ryan-Henry, J., & Huang, Y. (2016). A major increase in winter snowfall during the middle Holocene on western Greenland caused by reduced sea ice in Baffin Bay and the Labrador Sea: Holocene Sea Ice Loss Caused More Snow. *Geophysical Research Letters, 43*.

Thomas, E. K., Castañeda, I. S., McKay, N. P., Briner, J. P., Salacup, J. M., Nguyen, K. Q., & Schweinsberg, A. D. (2018). A Wetter Arctic Coincident With Hemispheric Warming 8,000 Years Ago. *Geophysical Research Letters, 45*(19), 10,637-610,647. https://agupubs.onlinelibrary.wiley.com/doi/abs/10.1029/2018GL079517

Thomas, E. K., Hollister, K. V., Cluett, A. A., & Corcoran, M. C. (2020). Reconstructing Arctic Precipitation Seasonality Using Aquatic Leaf Wax δ2H in Lakes With Contrasting Residence Times. *Paleoceanography and Paleoclimatology, 35*.

Walcott-George, C. K., Balter-Kennedy, A., Briner, J. P., Schaefer, J. M., & Young, N. E. (2025). Glacial erosion and history of Inglefield Land, northwestern Greenland. *The Cryosphere, 19*(6), 2067-2086. https://tc.copernicus.org/articles/19/2067/2025/

Weidick, A., & Bennike, O. (2007). Quaternary glaciation history and glaciology of Jakobshavn Isbræ and the Disko Bugt region, West Greenland: a review. *GEUS Bulletin, 14*, 1-78. https://doi.org/10.34194/geusb.v14.4985

Woznick, H. (2024). *SheddingLight on Past Ice-Free Intervals in Northwest Greenland: Luminescence Dating of the Base of the Camp Century Ice Core.* (Master of Science (MS)), Utah State University, Retrieved from https://digitalcommons.usu.edu/etd2023/281/

Zhao, B., Castañeda, I. S., Bradley, R. S., Salacup, J. M., de Wet, G. A., Daniels, W. C., & Schneider, T. (2021). Development of an in situ branched GDGT calibration in Lake 578, southern Greenland. *Organic Geochemistry, 152*, 104168. https://www.sciencedirect.com/science/article/pii/S0146638020302035

Zhao, B., Russell, J. M., Tsai, V. C., Blaus, A., Parish, M. C., Liang, J., et al. (2023). Evaluating global temperature calibrations for lacustrine branched GDGTs: Seasonal variability, paleoclimate implications, and future directions. *Quaternary Science Reviews, 310*, 108124. https://www.sciencedirect.com/science/article/pii/S0277379123001725

References From the Supporting Information

References

https://doi.org/10.5194/egusphere-2026-2378
Preprint. Discussion started: 5 May 2026
© Author(s) 2026. CC BY 4.0 License.

Acharya, S., Cluett, A. A., Grogan, A. L., Briner, J. P., Castañeda, I. S., & Thomas, E. K. (2025). Holocene temperatures in southwestern Greenland controlled by topography, ice sheet proximity and oceanic conditions. *EGUsphere, 2025*, 1-32. https://egusphere.copernicus.org/preprints/2025/egusphere-2025-3113/

Andersen, K. K., Azuma, N., Barnola, J. M., Bigler, M., Biscaye, P., Caillon, N., et al. (2004). High-resolution record of Northern Hemisphere climate extending into the last interglacial period. *Nature, 431*(7005), 147-151. https://doi.org/10.1038/nature02805

Atti, S., Bennike, O., & Weckström, K. (2024). Cladocerans and diatoms from an Early Pleistocene interglacial deposit at Pingorsuit, North-West Greenland. *Journal of Paleolimnology, 72*(3), 331-341. https://doi.org/10.1007/s10933-024-00333-z

Axford, Y., de Vernal, A., & Osterberg, E. C. (2021). Past Warmth and Its Impacts During the Holocene Thermal Maximum in Greenland. *Annual Review of Earth and Planetary Sciences, 49*(Volume 49, 2021), 279-307. https://www.annualreviews.org/content/journals/10.1146/annurev-earth-081420-063858

Axford, Y., Lasher, G. E., Kelly, M. A., Osterberg, E. C., Landis, J., Schellinger, G. C., et al. (2019). Holocene temperature history of northwest Greenland – With new ice cap constraints and chironomid assemblages from Deltasø. *Quaternary Science Reviews, 215*, 160-172. https://www.sciencedirect.com/science/article/pii/S0277379119302021

Axford, Y., Levy, L. B., Kelly, M. A., Francis, D. R., Hall, B. L., Langdon, P. G., & Lowell, T. V. (2017). Timing and magnitude of early to middle Holocene warming in East Greenland inferred from chironomids. *Boreas, 46*(4), 678-687. https://onlinelibrary.wiley.com/doi/abs/10.1111/bor.12247

Axford, Y., Losee, S., Briner, J. P., Francis, D. R., Langdon, P. G., & Walker, I. R. (2013). Holocene temperature history at the western Greenland Ice Sheet margin reconstructed from lake sediments. *Quaternary Science Reviews, 59*, 87-100. https://www.sciencedirect.com/science/article/pii/S0277379112004209

Balascio, N. L., D'Andrea, W. J., Bradley, R. S., & Perren, B. B. (2013). Biogeochemical evidence for hydrologic changes during the Holocene in a lake sediment record from southeast Greenland. *The Holocene, 23*(10), 1428-1439. https://doi.org/10.1177/0959683613493938

Bennike, O. (1990). The Kap København Formation: stratigraphy and palaeobotany of a Plio-Pleistocene sequence in Peary Land, North Greenland. *Meddelelser om Grønland. Geoscience, 23*, 85 pp. https://tidsskrift.dk/meddrgroenland_geosci/article/view/141978

Bennike, O. (2000). Palaeoecological studies of Holocene lake sediments from west Greenland. *Palaeogeography, Palaeoclimatology, Palaeoecology, 155*(3), 285-304. https://www.sciencedirect.com/science/article/pii/S0031018299001212

Bennike, O., Abrahamsen, N., Bak, M., Israelson, C., Konradi, P., Matthiessen, J., & Witkowski, A. (2002). A multi-proxy study of Pliocene sediments from Île de France, North-East Greenland. *Palaeogeography, Palaeoclimatology, Palaeoecology, 186*(1), 1-23. https://www.sciencedirect.com/science/article/pii/S003101820200439X

https://doi.org/10.5194/egusphere-2026-2378
Preprint. Discussion started: 5 May 2026
© Author(s) 2026. CC BY 4.0 License.

Bennike, O., & Böcher, J. (1992). Early Weichselian interstadial land biotas at Thule, Northwest Greenland. *Boreas, 21*(2), 111-118. https://onlinelibrary.wiley.com/doi/abs/10.1111/j.1502-3885.1992.tb00019.x

Bennike, O., & Böcher, J. (1994). Land biotas of the last interglacial/glacial cycle on Jameson Land, East Greenland. *Boreas, 23*(4), 479-487. https://onlinelibrary.wiley.com/doi/abs/10.1111/j.1502-3885.1994.tb00615.x

Bennike, O., Colgan, W., Hedenäs, L., Heiri, O., Lemdahl, G., Wiberg-Larsen, P., et al. (2023). An Early Pleistocene interglacial deposit at Pingorsuit, North-West Greenland. *Boreas, 52*(1), 27-41. https://onlinelibrary.wiley.com/doi/abs/10.1111/bor.12596

Bennike, O., Knudsen, K. L., Abrahamsen, N., Böcher, J., Cremer, H., & Wagner, B. (2010). Early Pleistocene sediments on Store Koldewey, northeast Greenland. *Boreas, 39*(3), 603-619. https://onlinelibrary.wiley.com/doi/abs/10.1111/j.1502-3885.2010.00147.x

Berke, M. A., Cartagena Sierra, A., Bush, R., Cheah, D., & O'Connor, K. (2019). Controls on leaf wax fractionation and δ2H values in tundra vascular plants from western Greenland. *Geochimica et Cosmochimica Acta, 244*, 565-583. https://www.sciencedirect.com/science/article/pii/S0016703718306069

Bierman, P. R., Christ, A. J., Collins, C. M., Mastro, H. M., Souza, J., Blard, P. H., et al. (2024). Scientific history, sampling approach, and physical characterization of the Camp Century sub-glacial sediment core, a rare archive from beneath the Greenland Ice Sheet. *EGUsphere, 2024*, 1-28. https://egusphere.copernicus.org/preprints/2024/egusphere-2023-2922/

Blaga, C. I., Reichart, G.-J., Heiri, O., & Sinninghe Damsté, J. S. (2009). Tetraether membrane lipid distributions in water-column particulate matter and sediments: a study of 47 European lakes along a north–south transect. *Journal of Paleolimnology, 41*(3), 523-540. https://doi.org/10.1007/s10933-008-9242-2

Bowen, G. (2017). The Online Isotopes in Precipitation Calculator. Retrieved from http://www.waterisotopes.org

Bowen, G. J., Wassenaar, L. I., & Hobson, K. A. (2005). Global application of stable hydrogen and oxygen isotopes to wildlife forensics. *Oecologia, 143*(3), 337-348. https://doi.org/10.1007/s00442-004-1813-y

Briner, J. P., McKay, N. P., Axford, Y., Bennike, O., Bradley, R. S., de Vernal, A., et al. (2016). Holocene climate change in Arctic Canada and Greenland. *Quaternary Science Reviews, 147*, 340-364. https://www.sciencedirect.com/science/article/pii/S0277379116300427

Brodersen, K. P., & Bennike, O. (2003). Interglacial Chironomidae (Diptera) from Thule, Northwest Greenland: matching modern analogues to fossil assemblages. *Boreas, 32*(4), 560-565. https://onlinelibrary.wiley.com/doi/abs/10.1111/j.1502-3885.2003.tb01235.x

Buizert, C., Keisling, B. A., Box, J. E., He, F., Carlson, A. E., Sinclair, G., & DeConto, R. M. (2018). Greenland-Wide Seasonal Temperatures During the Last Deglaciation. *Geophysical Research Letters, 45*(4), 1905-1914. https://agupubs.onlinelibrary.wiley.com/doi/abs/10.1002/2017GL075601

https://doi.org/10.5194/egusphere-2026-2378
Preprint. Discussion started: 5 May 2026
© Author(s) 2026. CC BY 4.0 License.

CAVM Team (Cartographer). (2024). Raster Circumpolar Arctic Vegetation Map

Christ, A. J., Bierman, P. R., Schaefer, J. M., Dahl-Jensen, D., Steffensen, J. P., Corbett, L. B., et al. (2021). A multimillion-year-old record of Greenland vegetation and glacial history preserved in sediment beneath 1.4 km of ice at Camp Century. *Proceedings of the National Academy of Sciences, 118*(13), e2021442118. https://doi.org/10.1073/pnas.2021442118

Christ, A. J., Rittenour, T. M., Bierman, P. R., Keisling, B. A., Knutz, P. C., Thomsen, T. B., et al. (2023). Deglaciation of northwestern Greenland during Marine Isotope Stage 11. *Science, 381*(6655), 330-335. https://www.science.org/doi/abs/10.1126/science.ade4248

Clark, I. D., & Fritz, P. (1997). *Environmental Isotopes in Hydrogeology* (1st ed.). Boca Raton, FL: CRC Press.

Cluett, A. A., & Thomas, E. K. (2021). Summer warmth of the past six interglacials on Greenland. *Proceedings of the National Academy of Sciences, 118*(20), e2022916118. https://www.pnas.org/doi/abs/10.1073/pnas.2022916118

Cluett, A. A., Thomas, E. K., McKay, N. P., Cowling, O. C., Castañeda, I. S., & Morrill, C. (2023). Lake Dynamics Modulate the Air Temperature Variability Recorded by Sedimentary Aquatic Biomarkers: A Holocene Case Study From Western Greenland. *Journal of Geophysical Research: Biogeosciences, 128*(7), e2022JG007106. https://agupubs.onlinelibrary.wiley.com/doi/abs/10.1029/2022JG007106

Cluett, A. A., Thomas, E. K., Evans, S. M., & Keys, P. W. . (2021). Seasonal Variations in Moisture Origin Explain Spatial Contrast in Precipitation Isotope Seasonality on Coastal Western Greenland. *Journal of Geophysical Research: Biogeosciences, 126*(11).

Collins, C. M., Perdrial, N., Blard, P. H., Keulen, N., Mahaney, W. C., Mastro, H., et al. (2024). Characterization of the 1966 Camp Century Sub-Glacial Core: A Multiscale Analysis. *EGUsphere, 2024*, 1-33. https://egusphere.copernicus.org/preprints/2024/egusphere-2024-2194/

Cowling, O. C., Thomas, E. K., Svendsen, J. I., Mangerud, J., Haflidason, H., Regnéll, C., & Brendryen, J. (2022). Western Siberia experienced rapid shifts in moisture source and summer water balance during the last deglaciation and early Holocene. *Journal of Quaternary Science, 37*(5), 790-804. https://onlinelibrary.wiley.com/doi/abs/10.1002/jqs.3386

Dahl-Jensen, D., Albert, M. R., Aldahan, A., Azuma, N., Balslev-Clausen, D., Baumgartner, M., et al. (2013). Eemian interglacial reconstructed from a Greenland folded ice core. *Nature, 493*(7433), 489-494. https://doi.org/10.1038/nature11789

Dansgaard, W. (1964). Stable isotopes in precipitation. *Tellus, 16*(4), 436-468. https://onlinelibrary.wiley.com/doi/abs/10.1111/j.2153-3490.1964.tb00181.x

Dansgaard, W., Clausen, H. B., Gundestrup, N., Hammer, C. U., Johnsen, S. F., Kristinsdottir, P. M., & Reeh, N. (1982). A New Greenland Deep Ice Core. *Science, 218*(4579), 1273-1277. https://www.science.org/doi/abs/10.1126/science.218.4579.1273

https://doi.org/10.5194/egusphere-2026-2378
Preprint. Discussion started: 5 May 2026
© Author(s) 2026. CC BY 4.0 License.

Dansgaard, W., Johnsen, S. J., Møller, J., & Langway, C. C. (1969). One Thousand Centuries of Climatic Record from Camp Century on the Greenland Ice Sheet. *Science, 166*(3903), 377-381. https://www.science.org/doi/abs/10.1126/science.166.3903.377

De Jonge, C., Hopmans, E. C., Zell, C. I., Kim, J.-H., Schouten, S., & Sinninghe Damsté, J. S. (2014). Occurrence and abundance of 6-methyl branched glycerol dialkyl glycerol tetraethers in soils: Implications for palaeoclimate reconstruction. *Geochimica et Cosmochimica Acta, 141*, 97-112. https://www.sciencedirect.com/science/article/pii/S0016703714004141

Dion-Kirschner, H., McFarlin, J. M., Masterson, A. L., Axford, Y., & Osburn, M. R. (2020). Modern constraints on the sources and climate signals recorded by sedimentary plant waxes in west Greenland. *Geochimica et Cosmochimica Acta, 286*, 336-354. https://www.sciencedirect.com/science/article/pii/S0016703720304579

Ellehoj, M. D., Steen-Larsen, H. C., Johnsen, S. J., & Madsen, M. B. (2013). Ice-vapor equilibrium fractionation factor of hydrogen and oxygen isotopes: Experimental investigations and implications for stable water isotope studies. *Rapid Communications in Mass Spectrometry, 27*(19), 2149-2158. https://analyticalsciencejournals.onlinelibrary.wiley.com/doi/abs/10.1002/rcm.6668

Fausto, R. S., Ahlstrøm, A. P., Van As, D., Bøggild, C. E., & Johnsen, S. J. (2009). A new present-day temperature parameterization for Greenland. *Journal of Glaciology, 55*(189), 95-105. https://www.cambridge.org/core/product/A4C890F114971EF99BF0EF46140C8382

Gao, L., Edwards, E. J., Zeng, Y., & Huang, Y. (2014). Major Evolutionary Trends in Hydrogen Isotope Fractionation of Vascular Plant Leaf Waxes. *PLoS ONE, 9*(11), e122610.

Gao, L., Hou, J., Toney, J., MacDonald, D., & Huang, Y. (2011). Mathematical modeling of the aquatic macrophyte inputs of mid-chain n-alkyl lipids to lake sediments: Implications for interpreting compound specific hydrogen isotopic records. *Geochimica et Cosmochimica Acta, 75*(13), 3781-3791. https://www.sciencedirect.com/science/article/pii/S0016703711002274

Gimeno, L., Eiras-Barca, J., Durán-Quesada, A. M., Dominguez, F., van der Ent, R., Sodemann, H., et al. (2021). The residence time of water vapour in the atmosphere. *Nature Reviews Earth & Environment, 2*(8), 558-569. https://doi.org/10.1038/s43017-021-00181-9

Gorbey, D. B., Thomas, E. K., Sauer, P. E., Raynolds, M. K., Miller, G. H., Corcoran, M. C., et al. (2022). Modern Eastern Canadian Arctic Lake Water Isotopes Exhibit Latitudinal Patterns in Inflow Seasonality and Minimal Evaporative Enrichment. *Paleoceanography and Paleoclimatology, 37*(5), e2021PA004384. https://agupubs.onlinelibrary.wiley.com/doi/abs/10.1029/2021PA004384

Grootes, P. M., & Stuiver, M. (1997). Oxygen 18/16 variability in Greenland snow and ice with 10−3- to 105-year time resolution. *Journal of Geophysical Research: Oceans, 102*(C12), 26455-26470. https://agupubs.onlinelibrary.wiley.com/doi/abs/10.1029/97JC00880

Grootes, P. M., & Stuiver, M. (1999). *GISP2 Oxygen Isotope Data (1 year averages)*. Retrieved from: https://doi.org/10.1594/PANGAEA.55532

https://doi.org/10.5194/egusphere-2026-2378
Preprint. Discussion started: 5 May 2026
© Author(s) 2026. CC BY 4.0 License.

Guo, J., Glendell, M., Meersmans, J., Kirkels, F., Middelburg, J. J., & Peterse, F. (2020). Assessing branched tetraether lipids as tracers of soil organic carbon transport through the Carminowe Creek catchment (southwest England). *Biogeosciences, 17*(12), 3183-3201. https://bg.copernicus.org/articles/17/3183/2020/

Hedenäs, L. (1994). Bryophytes from the last interglacial/glacial cycle, Jameson Land, East Greenland. *Boreas, 23*(4), 488-494. https://onlinelibrary.wiley.com/doi/abs/10.1111/j.1502-3885.1994.tb00616.x

Hedenäs, L., & Bennike, O. (2003). Moss Remains from the Last Interglacial at Thule, NW Greenland. *Lindbergia, 28*(2), 52-58. http://www.jstor.org/stable/20150125

Hersbach, H., Bell, B., Berrisford, P., Hirahara, S., Horányi, A., Muñoz-Sabater, J., et al. (2020). The ERA5 global reanalysis. *Quarterly Journal of the Royal Meteorological Society, 146*(730), 1999-2049. https://rmets.onlinelibrary.wiley.com/doi/abs/10.1002/qj.3803

Hollister, K. V., Thomas, E. K., Raynolds, M. K., Bültmann, H., Raberg, J. H., Miller, G. H., & Sepúlveda, J. (2022). Aquatic and Terrestrial Plant Contributions to Sedimentary Plant Waxes in a Modern Arctic Lake Setting. *Journal of Geophysical Research: Biogeosciences, 127*(8), e2022JG006903. https://agupubs.onlinelibrary.wiley.com/doi/abs/10.1029/2022JG006903

Hopmans, E. C., Schouten, S., & Sinninghe Damsté, J. S. (2016). The effect of improved chromatography on GDGT-based palaeoproxies. *Organic Geochemistry, 93*, 1-6. https://www.sciencedirect.com/science/article/pii/S0146638015002387

Huguet, C., Hopmans, E. C., Febo-Ayala, W., Thompson, D. H., Sinninghe Damsté, J. S., & Schouten, S. (2006). An improved method to determine the absolute abundance of glycerol dibiphytanyl glycerol tetraether lipids. *Organic Geochemistry, 37*(9), 1036-1041. https://www.sciencedirect.com/science/article/pii/S0146638006001094

IAEA/WMO. (2015). *Global Network of Isotopes in Precipitation (GNIP) Database* [data set]. Retrieved from: http://www.iaea.org/water

Johnsen, S. J., Clausen, H. B., Dansgaard, W., Gundestrup, N. S., Hammer, C. U., Andersen, U., et al. (1997). The δ18O record along the Greenland Ice Core Project deep ice core and the problem of possible Eemian climatic instability. *Journal of Geophysical Research: Oceans, 102*(C12), 26397-26410. https://agupubs.onlinelibrary.wiley.com/doi/abs/10.1029/97JC00167

Kobashi, T., Menviel, L., Jeltsch-Thömmes, A., Vinther, B. M., Box, J. E., Muscheler, R., et al. (2017). Volcanic influence on centennial to millennial Holocene Greenland temperature change. *Scientific Reports, 7*(1), 1441. https://doi.org/10.1038/s41598-017-01451-7

Koerner, R., & Russell, R. D. (1979). δ18O variations in snow on the Devon Island ice cap, Northwest Territories, Canada. *Canadian Journal of Earth Sciences, 16*(7), 1419-1427. https://cdnsciencepub.com/doi/abs/10.1139/e79-126

Kusch, S., Bennike, O., Wagner, B., Lenz, M., Steffen, I., & Rethemeyer, J. (2019). Holocene environmental history in high-Arctic North Greenland revealed by a combined biomarker and macrofossil approach. *Boreas, 48*(2), 273-286. https://onlinelibrary.wiley.com/doi/abs/10.1111/bor.12377

https://doi.org/10.5194/egusphere-2026-2378
Preprint. Discussion started: 5 May 2026
© Author(s) 2026. CC BY 4.0 License.

Lasher, G. E., Axford, Y., McFarlin, J. M., Kelly, M. A., Osterberg, E. C., & Berkelhammer, M. B. (2017). Holocene temperatures and isotopes of precipitation in Northwest Greenland recorded in lacustrine organic materials. *Quaternary Science Reviews, 170*, 45-55. https://www.sciencedirect.com/science/article/pii/S0277379116305650

Lee, H., Feakins, S. J., Lu, Z., Schimmelmann, A., Sessions, A. L., Tierney, J. E., & Williams, T. J. (2017). Comparison of three methods for the methylation of aliphatic and aromatic compounds. *Rapid Commun Mass Spectrom, 31*(19), 1633-1640.

Lindberg, K. R., Daniels, W. C., Castañeda, I. S., & Brigham-Grette, J. (2022). Biomarker proxy records of Arctic climate change during the Mid-Pleistocene transition from Lake El'gygytgyn (Far East Russia). *Clim. Past, 18*(3), 559-577. https://cp.copernicus.org/articles/18/559/2022/

Majoube, M. (1971). Fractionnement en oxygène 18 et en deutérium entre l'eau et sa vapeur. *J. Chim. Phys., 68*, 1423-1436. https://doi.org/10.1051/jcp/1971681423

Martin, K. C., Buizert, C., Brook, E., Williams, O. L., Edwards, J. S., Riddell-Young, B., et al. (2024). Greenland Ice Cores Reveal a South-To-North Difference in Holocene Thermal Maximum Timings. *Geophysical Research Letters, 51*(24), e2024GL111405. https://agupubs.onlinelibrary.wiley.com/doi/abs/10.1029/2024GL111405

Martínez-Sosa, P., Tierney, J. E., Stefanescu, I. C., Dearing Crampton-Flood, E., Shuman, B. N., & Routson, C. (2021). A global Bayesian temperature calibration for lacustrine brGDGTs. *Geochimica et Cosmochimica Acta, 305*, 87-105. https://www.sciencedirect.com/science/article/pii/S0016703721002635

McFarlin, J. M., Axford, Y., Kusch, S., Masterson, A. L., Lasher, G. E., & Osburn, M. R. (2023). Aquatic plant wax hydrogen and carbon isotopes in Greenland lakes record shifts in methane cycling during past Holocene warming. *Science Advances, 9*(39), eadh9704. https://www.science.org/doi/abs/10.1126/sciadv.adh9704

McFarlin, J. M., Axford, Y., Osburn, M. R., Kelly, M. A., Osterberg, E. C., & Farnsworth, L. B. (2018). Pronounced summer warming in northwest Greenland during the Holocene and Last Interglacial. *Proceedings of the National Academy of Sciences, 115*(25), 6357-6362. https://www.pnas.org/doi/abs/10.1073/pnas.1720420115

Morlighem, M., Williams, C. N., Rignot, E., An, L., Arndt, J. E., Bamber, J. L., et al. (2017). BedMachine v3: Complete Bed Topography and Ocean Bathymetry Mapping of Greenland From Multibeam Echo Sounding Combined With Mass Conservation. *Geophysical Research Letters, 44*(21), 11,051-011,061. https://agupubs.onlinelibrary.wiley.com/doi/abs/10.1002/2017GL074954

Naafs, B. D. A., Inglis, G. N., Zheng, Y., Amesbury, M. J., Biester, H., Bindler, R., et al. (2017). Introducing global peat-specific temperature and pH calibrations based on brGDGT bacterial lipids. *Geochimica et Cosmochimica Acta, 208*, 285-301. https://www.sciencedirect.com/science/article/pii/S0016703717300522

Nichols, J., Booth, R. K., Jackson, S. T., Pendall, E. G., & Huang, Y. (2010). Differential hydrogen isotopic ratios of Sphagnum and vascular plant biomarkers in ombrotrophic peatlands as a quantitative proxy for precipitation—evaporation balance. *Geochimica et Cosmochimica Acta, 74*(4), 1407-1416. https://www.sciencedirect.com/science/article/pii/S001670370900711X

https://doi.org/10.5194/egusphere-2026-2378
Preprint. Discussion started: 5 May 2026
© Author(s) 2026. CC BY 4.0 License.

O'Connor, K. F., Berke, M. A., & Ziolkowski, L. A. (2020). Hydrogen isotope fractionation in modern plants along a boreal-tundra transect in Alaska. *Organic Geochemistry, 147*, 104064. https://www.sciencedirect.com/science/article/pii/S0146638020300991

Otiniano, G. A., Porter, T. J., Buceta, R. E., Bergman, M. E., & Phillips, M. A. (2023). Climatic and environmentally driven variability in lacustrine brGDGT distributions at local to regional scales in Alaska and northwestern Canada. *Organic Geochemistry, 181*, 104604. https://www.sciencedirect.com/science/article/pii/S0146638023000505

Otiniano, G. A., Porter, T. J., Phillips, M. A., Juutinen, S., Weckström, J. B., & Heikkilä, M. P. (2024). Reconstructing warm-season temperatures using brGDGTs and assessing biases in Holocene temperature records in northern Fennoscandia. *Quaternary Science Reviews, 329*, 108555. https://www.sciencedirect.com/science/article/pii/S0277379124000568

Paxman, G. J. G., Austermann, J., & Hollyday, A. (2022). Total isostatic response to the complete unloading of the Greenland and Antarctic Ice Sheets. *Scientific Reports, 12*(1), 11399. https://doi.org/10.1038/s41598-022-15440-y

Poage, M. A., & Chamberlain, C. P. (2001). Empirical Relationships Between Elevation and the Stable Isotope Composition of Precipitation and Surface Waters: Considerations for Studies of Paleoelevation Change. *American Journal of Science, 301*(1), 1-15.

Raberg, J. H., Harning, D. J., Crump, S. E., de Wet, G., Blumm, A., Kopf, S., et al. (2021). Revised fractional abundances and warm-season temperatures substantially improve brGDGT calibrations in lake sediments. *Biogeosciences, 18*(12), 3579-3603. https://bg.copernicus.org/articles/18/3579/2021/

Raynolds, M. K., Walker, D. A., Balser, A., Bay, C., Campbell, M., Cherosov, M. M., et al. (2019). A raster version of the Circumpolar Arctic Vegetation Map (CAVM). *Remote Sensing of Environment, 232*, 111297. https://www.sciencedirect.com/science/article/pii/S0034425719303165

Russell, J. M., Hopmans, E. C., Loomis, S. E., Liang, J., & Sinninghe Damsté, J. S. (2018). Distributions of 5- and 6-methyl branched glycerol dialkyl glycerol tetraethers (brGDGTs) in East African lake sediment: Effects of temperature, pH, and new lacustrine paleotemperature calibrations. *Organic Geochemistry, 117*, 56-69. https://www.sciencedirect.com/science/article/pii/S0146638017304394

Sachse, D., Isabelle, B., Bowen, G., Chikaraishi, Y., Dawson, T., Feakins, S., et al. (2012). Molecular Paleohydrology: Interpreting the Hydrogen-Isotopic Composition of Lipid Biomarkers from Photosynthesizing Organisms. *Annual Review of Earth and Planetary Sciences, 40*, 221-249.

Schneider, T., Castañeda, I. S., Zhao, B., Krüger, S., Salacup, J. M., & Bradley, R. S. (2024). Tracing Holocene temperatures and human impact in a Greenlandic Lake: Novel insights from hyperspectral imaging and lipid biomarkers. *Quaternary Science Reviews, 339*, 108851. https://www.sciencedirect.com/science/article/pii/S0277379124003524

Schouten, S., Hopmans, E. C., & Sinninghe Damsté, J. S. (2013). The organic geochemistry of glycerol dialkyl glycerol tetraether lipids: A review. *Organic Geochemistry, 54*, 19-61. https://www.sciencedirect.com/science/article/pii/S0146638012001982

https://doi.org/10.5194/egusphere-2026-2378
Preprint. Discussion started: 5 May 2026
© Author(s) 2026. CC BY 4.0 License.

Schüpbach, S., Fischer, H., Bigler, M., Erhardt, T., Gfeller, G., Leuenberger, D., et al. (2018). Greenland records of aerosol source and atmospheric lifetime changes from the Eemian to the Holocene. *Nature Communications, 9*(1), 1476. https://doi.org/10.1038/s41467-018-03924-3

Stuiver, M., & Grootes, P. M. (2000). GISP2 Oxygen Isotope Ratios. *Quaternary Research, 53*(3), 277-284. https://www.sciencedirect.com/science/article/pii/S0033589400921276

Thomas, E., Briner, J., Ryan-Henry, J., & Huang, Y. (2016). A major increase in winter snowfall during the middle Holocene on western Greenland caused by reduced sea ice in Baffin Bay and the Labrador Sea: Holocene Sea Ice Loss Caused More Snow. *Geophysical Research Letters, 43*.

Thomas, E. K., Castañeda, I. S., McKay, N. P., Briner, J. P., Salacup, J. M., Nguyen, K. Q., & Schweinsberg, A. D. (2018). A Wetter Arctic Coincident With Hemispheric Warming 8,000 Years Ago. *Geophysical Research Letters, 45*(19), 10,637-610,647. https://agupubs.onlinelibrary.wiley.com/doi/abs/10.1029/2018GL079517

Thomas, E. K., Hollister, K. V., Cluett, A. A., & Corcoran, M. C. (2020). Reconstructing Arctic Precipitation Seasonality Using Aquatic Leaf Wax δ2H in Lakes With Contrasting Residence Times. *Paleoceanography and Paleoclimatology, 35*.

Vinther, B. M., Buchardt, S. L., Clausen, H. B., Dahl-Jensen, D., Johnsen, S. J., Fisher, D. A., et al. (2009). Holocene thinning of the Greenland ice sheet. *Nature, 461*(7262), 385-388. https://doi.org/10.1038/nature08355

Zhao, B., Russell, J. M., Tsai, V. C., Blaus, A., Parish, M. C., Liang, J., et al. (2023). Evaluating global temperature calibrations for lacustrine branched GDGTs: Seasonal variability, paleoclimate implications, and future directions. *Quaternary Science Reviews, 310*, 108124. https://www.sciencedirect.com/science/article/pii/S0277379123001725